



MASTER THESIS, DUAL DIPLOMA PROGRAM  
ADVANCED LEVEL, 30 ECTS  
*STOCKHOLM - BEIJING, 2018*



# Measurement of Coating Thickness Based on Terahertz Time-Domain Spectroscopy (THz-TDS) Technology

Yiran Yu

TRITA-SCI-GRU 2018:062

TSINGHUA UNIVERSITY



KTH-ROYAL INSTITUTE OF TECHNOLOGY



# Measurement of Coating Thickness Based on Terahertz Time-Domain Spectroscopy (THz-TDS) Technology

Yiran Yu

Thesis Submitted to

Tsinghua University  
In partial fulfilment of the requirement  
for the degree of  
Master of Engineering  
In  
Nuclear Energy and Nuclear Technology  
Engineering

KTH Royal Institute of Technology  
In partial fulfilment of the requirement  
for the degree of  
Master of Science  
In  
Engineering Physics

Co-supervisor: Associate Professor  
Yingxin Wang  
Department of Engineering Physics

Co-supervisor: Professor  
Fredrik Laurell  
Department of Applied Physics

UNDER THE COOPERATION AGREEMENT ON DUAL MASTER'S  
DEGREE PROGRAM IN NUCLEAR ENERGY RELATED DISCIPLINES

JUNE 2018 (Month Year)

# 关于学位论文使用授权的说明

## Statement on thesis usage authorization

本人完全了解清华大学有关保留、使用学位论文的规定，即：

清华大学拥有在著作权法规定范围内学位论文的使用权，其中包括：（1）已获学位的研究生必须按学校规定提交学位论文，学校可以采用影印、缩印或其他复制手段保存研究生上交的学位论文；（2）为教学和科研目的，学校可以将公开的学位论文作为资料在图书馆、资料室等场所供校内师生阅读，或在校园网上供校内师生浏览部分内容；（3）根据《中华人民共和国学位条例暂行实施办法》，向国家图书馆报送可以公开的学位论文。

本人保证遵守上述规定。

（保密的论文在解密后遵守此规定）

I entirely understand Tsinghua University policies concerning reserving and using copies of graduate theses. That is, the university has the right to distribute a copy of the thesis and allow students to read and borrow it. The university may publicise the whole or part of the thesis content and distribute the thesis by means of filming, microfilming or any other duplication methods.

(Any confidential thesis must also fully comply with this policy following declassification)

作者签名：

导师签名：

日 期：

日 期：

## 摘 要

太赫兹辐射有许多优良特性。第一，太赫兹辐射对多数介电材料有良好的穿透性，例如纸张、塑料、涂层和泡沫。第二，很多有机物的太赫兹光谱具有独特的特征。第三，太赫兹辐射是非电离辐射，对人体安全。因此，得益于这些特点，太赫兹技术迅速发展。利用太赫兹辐射的穿透性可以进行无损检测。利用不同物质对太赫兹辐射的响应具有独特光谱特征的性质，可以通过太赫兹光谱来分析物质成分，如检测安全检查领域中的毒品、爆炸物等。

基于太赫兹时域光谱的涂层厚度测量方法是本文的主要研究内容。本文针对反射式太赫兹时域光谱测量基底上薄层厚度的问题，研究并提出了基于反射太赫兹光谱分析提取涂层折射率和厚度的方法。

本文对基底上覆盖有涂层的材料建模为多层材料，太赫兹波入射到材料并进行传播，利用菲涅尔公式描述太赫兹波在各界面的透射与反射过程，从而得到参考太赫兹信号和涂层反射太赫兹信号之间的关系，即传递函数的模型。实际测量时，传递函数中的材料参数和厚度是未知的，用太赫兹时域光谱仪可以测量出参考和反射太赫兹信号，算法通过差异进化算法迭代传递函数中的未知参数使得时域信号曲线最小二乘误差降低，而拟合得到传递函数模型中的未知参数，获取被测涂层的厚度。

之后，本文设计了一种反射式太赫兹时域光谱测量实验装置。通过该装置把太赫兹时域光谱仪中的太赫兹发射器和接收器架设成反射式测量布局，让太赫兹波从上方发射、接收，被测物体放置在下方升降平移台上，有效保证测量的准确性。再加上算法考虑了液体基底液面变化产生的相位误差，使测量水面油污厚度成为可能。实验通过使用这一装置，有效测量得到了钢板上的标签厚度和水上油污的厚度。

这项研究提供了基于反射式太赫兹时域光谱技术的厚度测量实用方法。此外，所开发的反射式测量实验装置扩展了太赫兹光谱的应用。

**关键词：**太赫兹时域光谱;涂层厚度测量;建模;拟合;相位误差

## **Abstract**

Radiation in the Terahertz range has many excellent features; therefore, terahertz applications have been developed widely over decades. Firstly, water, metal, and dielectric, appear different optical properties at terahertz frequencies. Water is highly absorptive in terahertz region, while metals are highly reflective. Thus, dried substances can be differentiated from moist ones. Metal objectives are easy to tell. Dielectrics, nonpolar and nonmetallic materials, are transparent to terahertz radiation, while usually opaque at visible wavelengths. Thus, terahertz spectroscopy can be applied to inspect sealed packages, since common packaging materials are dielectric. Secondly, there are numerous features such as large-amplitude vibrational motions of organic compounds. These characteristics can be exploited by terahertz spectroscopy for analyzing molecular composition, such as detection of drugs, explosive products in security check field. Besides, it is non-nucleonic and non-ionizing, namely safe.

The terahertz time-domain spectroscopy technology is a major research direction of for this project. This essay aims at determining the thickness of a thin layer on a reflective substrate. Methods to obtain the refractive index and layer thickness based on analysis of reflected terahertz wave are researched and presented.

Applications of terahertz spectroscopy on thickness measurements were researched. Simulations were applied to test and modify the algorithm. We model the sample as multi-layer material. Terahertz wave incident at the material, and the transmission and reflection at the interfaces are described by Fresnel equations. The relationship between incident radiation and reflected terahertz wave is the model of transfer function. The unknown parameters in the transfer function model are obtained by fitting the time-domain spectra curve, through which we get the thickness of the coating.

After that, a new experimental setup is designed. The terahertz transmitter and receiver of the spectrometer are mounted on a guide. Terahertz wave is emitted and detected from the top, and the sample is placed on a platform below. This setup ensures the accuracy of the measurements and broadens application range. By using this setup, we performed experiments to measure the thickness of a sticker on a steel plate and oil

on water. The uneven distribution of oil on the surface of the water causes changes in the liquid surface position. The algorithm innovatively introduces an unknown variable of the position of the liquid surface, making it possible to measure the thickness of oil contamination on the surface.

This research confirms the previous findings and gives us a practical method for reflective terahertz spectroscopy. Additionally, the experimental setup and the consideration of change in liquid surface level contribute to the existing modelling knowledge.

**Key words:** Terahertz time-domain spectroscopy; thickness; model; fitting; phase shift

## Table of Contents

<b>CHAPTER 1 INTRODUCTION AND MOTIVATION .....</b>	<b>1</b>
1.1 FEATURES OF TERAHERTZ RADIATION .....	1
1.2 TERAHERTZ TIME-DOMAIN SPECTROSCOPY (THZ-TDS) .....	2
1.2.1 Terahertz Generation .....	3
1.2.2 Terahertz Detection .....	4
1.2.3 Fiber-coupled terahertz spectrometer .....	5
1.3 APPLICATIONS ON THICKNESS MEASUREMENT.....	9
1.4 AIM OF THIS THESIS.....	12
<b>CHAPTER 2 THEORETICAL BACKGROUND .....</b>	<b>14</b>
2.1 SINGLE-LAYER MODEL .....	14
2.2 DOUBLE-LAYER MODEL.....	16
2.3 INCIDENT ANGLE .....	18
2.4 MODEL COMPLEX REFRACTIVE INDEX .....	18
2.5 DIFFERENTIAL EVOLUTION (DE) ALGORITHM.....	19
2.6 CONSIDERATIONS ABOUT SUBSTRATE WATER .....	20
<b>CHAPTER 3 SIMULATION.....</b>	<b>22</b>
3.1 SINGLE-LAYER MODEL .....	22
3.2 DOUBLE-LAYER MODEL.....	27
3.3 PHASE SHIFT.....	31
3.4 ANALYSIS.....	32
<b>CHAPTER 4 EXPERIMENTAL WORK.....</b>	<b>34</b>
4.1 EXPERIMENTAL SETUP.....	34
4.2 REFLECTIVE MEASUREMENT .....	35
4.2.1 Stickers on steel plate .....	35



4.2.2 Oil on water .....	38
<b>CHAPTER 5 RESULTS AND DISCUSSION .....</b>	<b>40</b>
5.1 STICKERS ON STEEL PLATE .....	40
5.2 OIL ON WATER .....	43
<b>CHAPTER 6 CONCLUSIONS AND PROPOSAL FOR FUTURE WORK.....</b>	<b>46</b>
<b>REFERENCES .....</b>	<b>48</b>
<b>ACKNOWLEDGEMENT .....</b>	<b>52</b>
<b>PERSONAL STATEMENT .....</b>	<b>53</b>
<b>RESUME .....</b>	<b>54</b>

## Chapter 1 Introduction and Motivation

### 1.1 Features of Terahertz Radiation

Terahertz (THz) radiation is electromagnetic radiation; its frequency lies between infrared and microwave. Radiation in the Terahertz range is typically defined as 0.1 – 10 THz, wavelength between 30  $\mu\text{m}$  and 3 mm. [1]

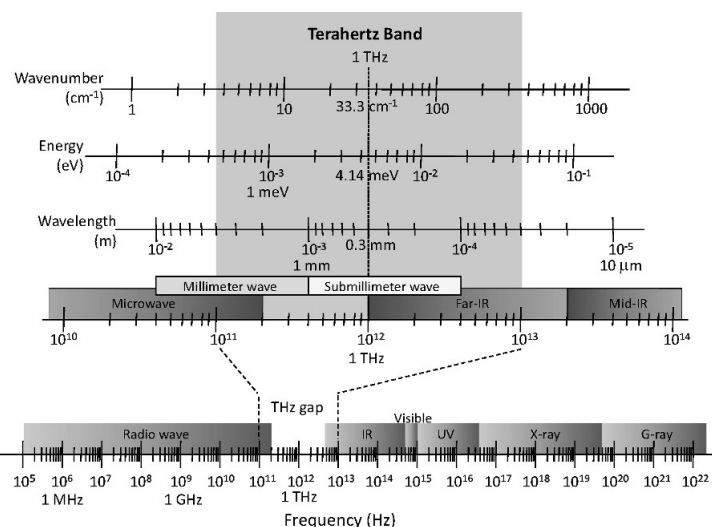


Figure 1. 1 Terahertz band in the electromagnetic spectrum [1]

Terahertz radiation has many excellent features. It penetrates through nearly all dielectric materials: paper, plastics, coatings, and foams. It has characteristic features for numerical organic materials. It is non-nucleonic and non-ionizing, namely safe. These features give rise to rapid progress of terahertz technology.

Firstly, three largely grouped condensed matter: water, metal, and most of other dielectric, appear different optical properties at terahertz frequencies. Water is highly absorptive in terahertz region, while metals are highly reflective. Most of dielectrics, nonpolar and nonmetallic materials, are penetrable to terahertz radiation, while usually opaque at visible wavelengths. Thus, terahertz spectroscopy can be applied to inspect sealed packages, since common packaging materials are dielectric. Non-destructive test is one of the important applications of terahertz spectroscopy.

Additionally, the molecular dynamics or lattice vibration occurs in time scale of picoseconds ( $10^{-12}$  s), which corresponds to THz frequencies. Therefore, material

responses to terahertz radiation appears spectral features. For example, absorption by water vapor shows spectral signatures in terahertz region; thus, dried substances can be differentiated from moist ones. Furthermore, there are numerous features such as large-amplitude vibrational motions of organic compounds. These characteristics can be exploited by terahertz spectroscopy for analyzing molecular composition, such as detection of drugs, explosive products in security check field.

## 1.2 Terahertz Time-Domain Spectroscopy (THz-TDS)

The terahertz time-domain spectroscopy technology is a major research direction of for this project. Broadband terahertz spectroscopy for scientific research is well-established with a growing number of techniques and applications. Typically, a broadband terahertz spectrometer adopts femtosecond laser to generate broad band spectra and detect terahertz pulses. [2] Coherent field detection yields high resolution time-domain spectra, from which both the amplitude and phase of terahertz spectra can be obtained.

In previous research phase, our research group has developed a terahertz time-domain spectrometer prototype successfully [3].

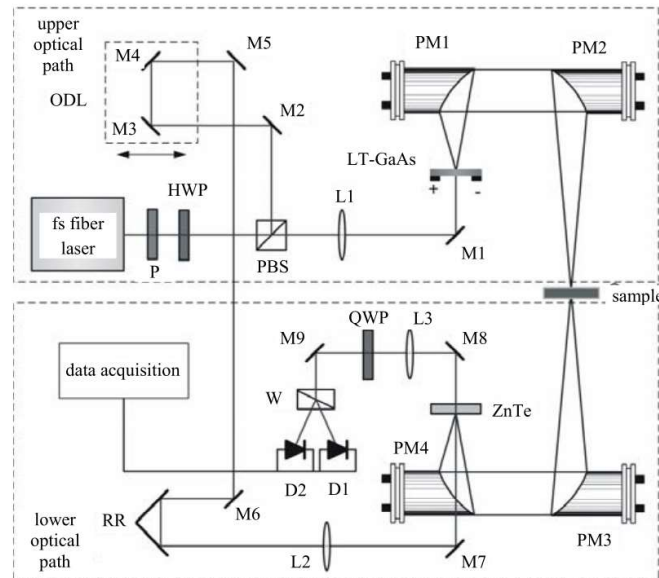


Figure 1. 2 Optical path schematic diagram of the portable THz time domain spectrometer [3]

This technology is pump-probe spectroscopy. A laser generates femto-second optical pulses. The optical beam is split into two by a beam splitter. The pump beam is

focused onto a photoconductive antenna, which generates terahertz pulses. An electro-optical crystal is set up to detect the terahertz signal passed through the specimen. The probe beam is guided to an optical delay line. Changing its length changes the arrival time of the detection pulse with respect to the Terahertz pulse at the detector. When repeating the measurement of the Terahertz field at the detector for a set of different delays, the Terahertz waveform is being sampled in its entirety.

### 1.2.1 Terahertz Generation

Generation of broadband terahertz radiation is the core of terahertz time-domain spectroscopy. There are typically two ways to generate broadband terahertz radiation.

One way is to exploit a nonlinear crystal where incident electromagnetic waves undergo nonlinear frequency conversion. [1] Femtosecond laser pulses generate broadband terahertz pulses via optical rectification.

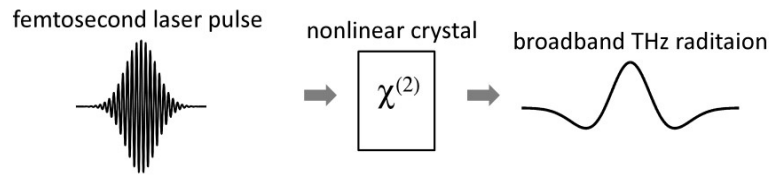


Figure 1. 3 Terahertz radiation from nonlinear crystal

Terahertz radiation can also be generated from a biased photoconductive antenna (PCA) excited by laser beams. A PCA consists of two metal electrodes on a semiconductor substrate. A direct current (DC) bias is applied between the electrodes. An optical beam generates photocarriers when the gap between the electrodes is illuminated, and the free carriers are accelerated by the static DC bias electrical field. Simultaneously, the charge density declines primarily by trapping of carriers in defect sites on the time scale of carrier lifetimes. The impulse current arising from the acceleration and decay of free carriers is the source of the sub picosecond pulses. This photocurrent varies in time corresponding to the incident laser beam intensity; consequently, it produces broadband Terahertz pulses. [1]

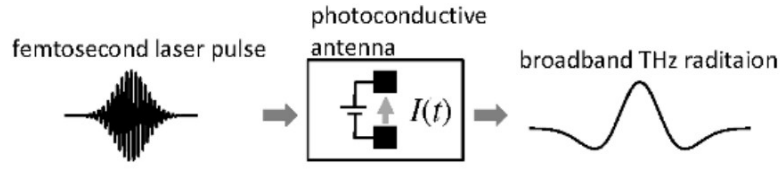
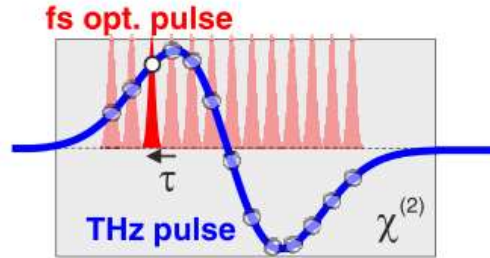


Figure 1. 4 Terahertz radiation from PCA

In this spectrometer developed by our laboratory, broadband terahertz radiation is generated by a photoconductive antenna.

### 1.2.2 Terahertz Detection

The detection of terahertz waves is an inverse process of terahertz wave generation. There are also two methods of electro-optic sampling detection and photo-conduction sampling detection using nonlinear crystals and photoconductive antennas. The pump-probe detection technique uses equivalent time sampling. One of the most attractive features of pump-probe terahertz spectroscopy is the ability to coherently detect the terahertz field, both amplitude and phase. This allows one not only to determine the absorption and dispersion properties of samples simultaneously, but also results in a far higher sensitivity/dynamic range compared to square-law (intensity) detection with a thermal detector or conventional photodiode. [2]

Figure 1. 5 Principle of time-domain sampling of a THz pulse using fs-optical gate pulses as a function of pulse delay  $\tau$  [2]

In our terahertz time-domain spectrometer, nonlinear crystals ZnTe is used for detection, employing the electro-optic Pockel's effect. Terahertz electric field induces an instantaneous birefringence [1] (difference in the refractive indices along each crystal axis) in the crystal, which leads to a change in the polarization state of the co-propagating optical pulse. A pair of photodetectors detects the difference between the two polarization optics and obtain the terahertz electric field intensity.

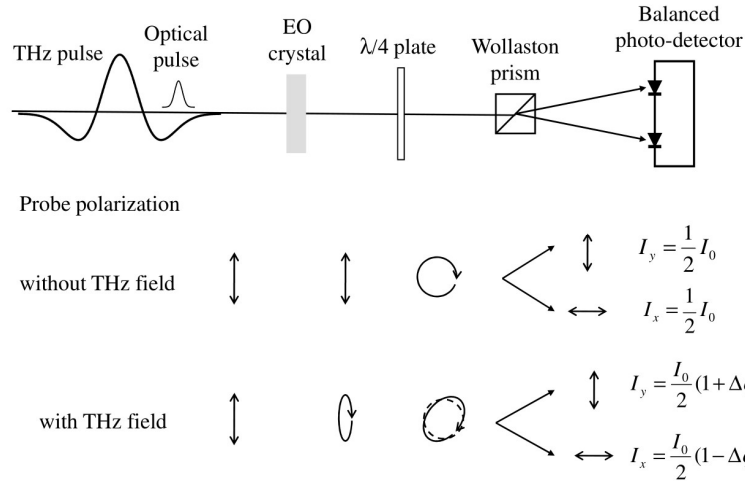


Figure 1. 6 Schematic diagram of a typical setup for free-space electro-optic sampling. Probe polarizations with and without a THz field are depicted before and after the polarization optics [1]

### 1.2.3 Fiber-coupled terahertz spectrometer

Researchers all over the world have a lot of research about fiber-coupled terahertz spectrometers.

As early as 2000, the world's first commercial Terahertz system T-Ray2000 came out, launched by the American company Picometrix. This system uses a mode-locked Ti:sapphire laser with a working wavelength of 750-850 nm to generate a laser pulse with a duration of 100 fs. The laser pulse is passed through the grating dispersion pre-compensation device twice to obtain a negative dispersion, and then passes through the fiber. Propagation illumination is applied to the photoconductive antenna. The optical delay line uses a delay device that moves in free space along a straight line. The time window of this system is 30 ps, the bandwidth can reach 0.03-3 THz, the scan rate can reach 22 Hz, and the resolution can reach 33 GHz. [4]

In 2007, Vieweg et al. [5] built a terahertz time-domain spectroscopy system on a 90\*90 cm vibration isolation optical platform in the laboratory. It can be used industrially by insulating the light path in an aluminium box to isolate dust. In the relatively compact system, a femtosecond Ti:sapphire laser with a working wavelength of 780 nm is also used. The laser pulse is subjected to a negative dispersion by the grating dispersion pre-compensation device, and then propagated through the optical fiber to the

photoconductive antenna. The optical delay line uses free space. A delay device that vibrates along a straight line. The signal to noise ratio of this system can reach 75 dB.

Frank Ellrich et al. [6] used optic fiber terahertz spectrometers with a laser whose center wavelength of 800 nm. They also pointed out that using 1.5  $\mu\text{m}$  wavelength lasers instead of 800 nm lasers can save costs and make the system more integrated.

Using a laser with a wavelength of 1.55  $\mu\text{m}$ , the antenna base material for the terahertz-wave emission needs to be changed, and the integration of the optical fiber and the overall layout of the system are also different.

The world's first all-fiber terahertz time-domain spectroscopy system using a 1.5  $\mu\text{m}$  wavelength laser was proposed by Sartorius et al. [7] in 2008. The key component that can be achieved in this way is the novel low-temperature growth InGaAs/InAlAs multilayer photoconductive antenna. The photoconductive antenna is incorporated into the module to achieve full fiber. The laser selected was Menlo Systems, and the laser wavelength was 1550 nm, and the duration was 100 fs. The JDS-Fitel HD4 was used as the delay line. The bandwidth they achieve is up to 3 THz.

The South Korean team of Sang-Pil Han and others focused on the generation of terahertz waves in response to 1.5  $\mu\text{m}$  wavelength lasers and the investigation of optical fiber-integrated photoconductive antenna modules, taking into account antenna structure, packaging, heat dissipation, and integration issues. [8] In 2011, a fiber-optic terahertz time-domain spectroscopy system was established by them. [9] The laser used was Menlo Systems. The laser pulse duration was 70 fs. The dispersion compensation fiber was used for negative dispersion pre-compensation. The bandwidth is 2 THz, and the resolution is 1.2 GHz.

In 2014, Vieweg et al. built a fiber-based terahertz time-domain spectroscopy system with a peak dynamic range of 90 dB, creating a new world record in commercial systems. [10] The optical delay line is a motor-driven corner cube prism, with a 4-fold optical path that can reach 3000 ps delay. The laser used was Toptica FemtoFERb 1560. The laser pulses emitted were also subjected to negative dispersion pre-compensation via a dispersion-compensating fiber. The photoconductive antenna used a low-temperature

growth InGaAs/InAlAs multilayer photoconductive antenna, the bandwidth can reach 4.5 THz. The system is packaged in a 48\*40\*20 cm box and is compact.

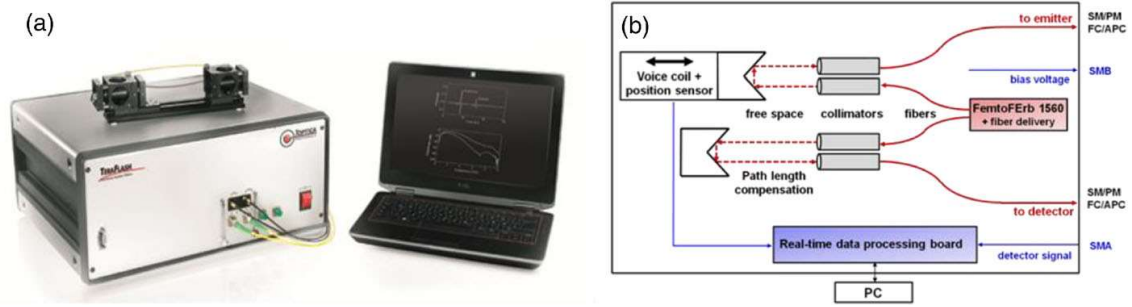


Figure 1. 7 TOPTICA terahertz spectrometer. [10]

In 2017, K. Merghem et al. replaced the expensive fiber-optic femtosecond lasers with relatively low-cost monolithic semiconductor lasers and established a fiber-optic terahertz time-domain spectroscopy system. [11] The operating wavelength of this system is 1550 nm, which achieves a bandwidth of 0.6 THz and a signal-to-noise ratio of 45 dB.

Fiber-optic terahertz time-domain spectroscopy systems not only exist in the laboratory but have also entered the international market.

Picometrix, who introduced the world's first commercially available T-Ray system T-Ray 2000, has already introduced T-Ray 5000. By using optical fiber, it has been made more compact on the basis of the original, and it has moved from the laboratory into industrial applications. The frequency bandwidth has also increased, and the sampling rate has reached 1 kHz, which has been declared the fastest in the world. [12]

Fiber-optic terahertz time-domain spectrometers sold in the international market include TeraView (UK) TeraPulse 4000 [13], Ekspla (Lithuania) T-FIBER series [14] and Menlo (Germany) Tera K15 [15], TeraFlash of Toptica (Germany) [16]. There are no uniform standards for these terahertz spectrometer products, and the technologies used are different. Therefore, the spectral range, resolution, dynamic range, and signal-to-noise ratio of the terahertz time-domain spectrometers are all different. We summarize these spectrometers in the following table.



Table 1. 1 Commercial Fiber Terahertz Time-Domain Spectrometer

	T-Ray 5000	TeraPulse 4000	TERA K15	T-FIBER series	TeraFlash
Time Group	2013 USA Picometrix	2015 UK TeraView	2014 Germany Menlo	2012 Lithuania Ekspla	2014 Germany Toptica
Laser	Ti: Sapphire	Ti: Sapphire	Er-doped fiber laser T-Light FC	Femto-second fiber laser LightWire FF50	Femto-second fiber laser FemtoERb THz FD 6.5
Wavelength Emitter and detector	800 nm Fiber coupled PCA	790 nm PCA	1560 nm Fiber coupled PCA	1064 nm Fiber coupled PCA	1560 nm Fiber coupled PCA
Time window	320 ps	1600 ps	>850 ps	110 ps	200 ps
Size	17.5*22*7 inches	702*645* 468 mm	540*450*2 00 mm	400*400*158 mm	180*450*560 mm
Bandwidth	0.2-2 THz	0.06-4 THz	4.5 THz	>3.5 THz	0.1-5 THz
SNR/DR	>70 dB	>4 OD	80 dB	>65 dB	>90 dB
Scan rate	100 or 1000 Hz	30 scans/s	200 waveforms /s	10 spectra/s	35 traces/s
Resolution	3.1 GHz	1.2 cm <sup>-1</sup>	< 1.2 GHz	< 10 GHz	<5 GHz

At present, the development trend of fiber-based terahertz time-domain spectroscopy systems is to use communication wavelengths of 1.5  $\mu\text{m}$  to replace 800 nm lasers, with a signal-to-noise ratio of 90 dB being the highest in the world, and a spectral acquisition rate of 1000 Hz being the fastest in the world. The structure has dropped to a personal computer case size. At present, the technology still has room for improvement in some aspects, such as how to improve the signal to noise ratio in the high frequency part of the terahertz spectrum and the detection sensitivity of the system. The next generation terahertz spectrometers will target at wide-spectrum terahertz development, such as terahertz sources of up to ten or even tens of terahertz, miniaturization of the core components of spectroscopic instruments, cost reduction, and suitability for various applications.

The key technology for the development of optic-fiber terahertz time-domain spectrometers is the new type of photoconductive antenna substrate material with short carrier lifetime, high mobility, and high dark resistivity. The photoconductive antenna structure, packaging, heat dissipation, and integration forms, appropriate dispersion compensation, precise control of optical delay lines, weak signal noise reduction measurement techniques, and miniaturization of core components.

### 1.3 Applications on Thickness Measurement

Terahertz spectroscopy applications have been developed widely over decades. As for thickness measurement, terahertz spectroscopy can be used on inspection of aeronautics composite material [17], adhesion quality [18], painting on automobiles [19], thermos isolating coating in nuclear industry, anti-rusting coating on pipes, coating on pills in pharmacy [20].

Tetsuo Fukuchi et al. measured thickness of the topcoat of a thermal barrier coating from the reflected terahertz waveforms. [21] They determined the thickness by the time interval between reflections. The principle is shown in Figure 1. 8. However, this method needs successive reflections, i.e. it has drawbacks when measuring very thin coatings.

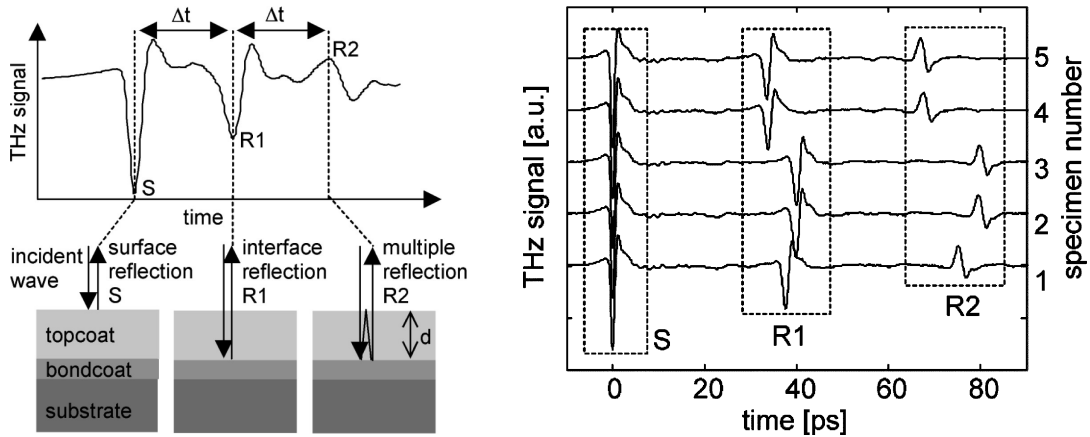


Figure 1. 8 Multiple reflections of terahertz waves in the topcoat and typical reflected waveform [21]

Masaaki Sudo et al. developed a non-destructive thickness measurement system in 2016 [22]. The system is mounted on a robot arm and applied to non-destructive measurement for multilayer paint thickness on automotive parts.

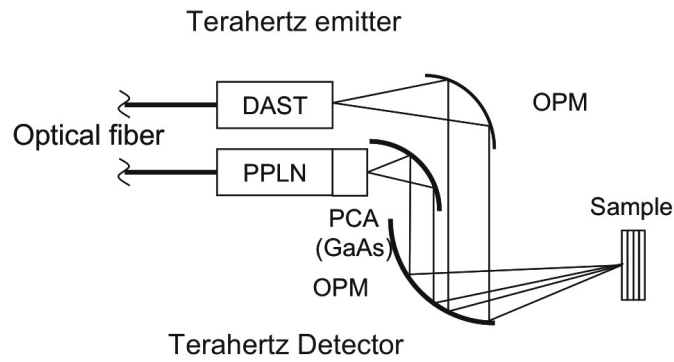


Figure 1. 9 Schematic of terahertz emitter and detector. A DAST crystal is used as the terahertz emitter and a PCA is used as the terahertz detector. OPM off-axis parabolic mirror, DAST 4-N,N-dimethylamino-4'-N'-methylstilbazolium tosylate, PPLN periodically poled lithium niobate, PCA photoconductive antenna [22]



Figure 1. 10 Multilayer paint measurement with the PMU mounted on a robot arm scanning [22]

They adopted terahertz time-of-flight thickness measurement method, taking advantage of the transparency of the materials used in automotive paint coats.

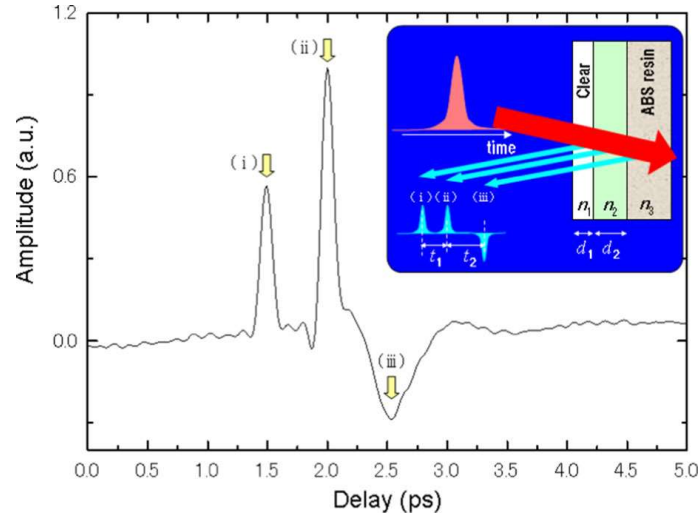


Figure 1. 11 Terahertz waveform reflected from a multilayer paint film [22]

Soufiene Krimi et al. introduced a self-calibration model [19], taking into consideration of the challenges in real industry. Their method could measure multi-layer wet on wet automotive painting during the process.

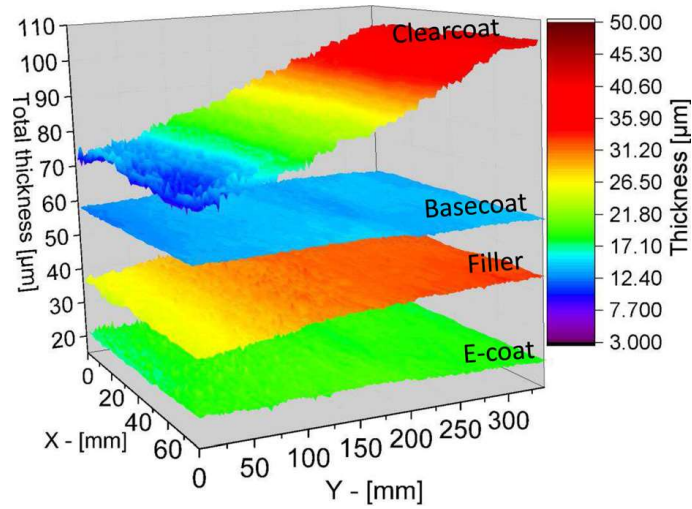


Figure 1. 12 A 3D thickness image of a four-layer specimen [19]

J. L. M. van Mechelen et al. proposed a novel terahertz analysis approach [23]. This method treats the specimen as stratified system and describes the interaction of each interface with a realistic way. It provides accurate thickness. They described the material well with Drude–Lorentz parameterization, while other methods are generally used. Analysis in advance is needed to decide.

Comparing to some traditional inspecting methods, terahertz spectroscopy has many advantages. Unlike ultrasound, eddy current, and induction, terahertz spectroscopy

is non-contact. [24] Furthermore, ultrasound, eddy current, induction, optic-thermal, and microwave are not applicable to multi-layer measurements. [25] Unlike x-ray or beta gauges, terahertz needs no radiation protection. Unlike optical coherence, terahertz can penetrate almost all dielectric materials. [26] The resolution of terahertz spectroscopy is higher than infra-red.

## **1.4 Aim of This Thesis**

This essay aims at determining the thickness of a thin layer on a reflective substrate.

First of all, terahertz radiation and terahertz time-domain spectroscopy was introduced. After that, methods to obtain the refractive index and layer thickness based on analysis of reflected terahertz wave are researched and presented in Chapter 1.

Chapter 2 provides the theoretical background of the multi-layer modelling of incidence and reflection of terahertz wave at the specimen. Methods and analysis are illustrated as well as the fitting algorithm. Terahertz wave incident at the multi-layered model, and the transmission and reflection at the interfaces are described by Fresnel equations. The relationship between incident radiation and reflected terahertz wave is the model of transfer function. The unknown parameters in the transfer function model are obtained by fitting the time-domain curve, through which we get the thickness of the coating. Differential evolution algorithm is adopted for fast convergence and vast range search.

Having this method, simulations to test and modify the algorithm are presented in Chapter 3. The simulation results prove the method applicable.

After that, a new experimental setup is designed and presented in Chapter 4. The terahertz transmitter and receiver of the spectrometer are mounted on a guide. Terahertz wave is emitted and detected from the top, and the sample is placed on a platform below. This setup ensures the accuracy of the measurements and broadens application range. By using the setup, experiments are done to verify the method and algorithm. We performed experiments to measure the thickness of a sticker on a steel plate and oil on water.

Chapter 5 gives the results and discussion. The results show that the error for measurement of the sticker is low, and the thickness change of oil film and water level over time is in accordance with the physical principle of buoyancy.

Finally, in Chapter 6, conclusions are drawn and following future works are mentioned. This research gives us a practical method for reflective terahertz spectroscopy. Additionally, the experimental setup and the consideration of change in liquid surface level contribute to the existing modelling knowledge. Both of them worth further investigation in the future.

## Chapter 2 Theoretical Background

The reflection of terahertz wave from the specimen can be detected by terahertz time-domain spectrometer. In this Chapter, we describe a terahertz thickness analysis approach, consist of multi-layer modelling, consideration of incident angle, a time-domain based fitting procedure, an algorithm for convergence, and considerations about phase shifting.

### 2.1 Single-Layer Model

We can model the specimen as a multi-layer material. [23] For the case of the bilayer material system shown in Figure 2. 1, with the angle of incidence  $\theta_i = 0$ , the reflected electric field  $E_r$  can be calculated using the incident electric field  $E_{r,0}$  and the transfer function of the entire multilayer structure  $T_0$  through

$$E_r(\omega) = T_0(\omega) \cdot E_{r,0}(\omega) \quad (2-1)$$

$$\begin{aligned} T_0(\omega) = & r_{12} + t_{12} \cdot r_{23} \cdot t_{21} \cdot e^{-i2\beta_2} \\ & + t_{12} \cdot r_{23} \cdot r_{21} \cdot r_{23} \cdot t_{21} \cdot e^{-i4\beta_2} \\ & + t_{12} \cdot r_{23} \cdot r_{21} \cdot r_{23} \cdot r_{21} \cdot r_{23} \cdot t_{21} \cdot e^{-i6\beta_2} + \dots \end{aligned} \quad (2-2)$$

Where,

$\beta_k = \omega n_k d_k / c$  is the phase shift accumulated in the layer k;

$\omega$  is the frequency of the radiation;

$\tilde{n}_k$  is the complex index of refraction of layer k, the definition is  $\tilde{n}_k = n_k - jk_k$ ;

$d_k$  is the thickness of layer k;

$c$  is the speed of light in vacuum;

the transmission  $t_{ij}$  and reflection  $r_{ij}$  coefficients are:

$$t_{ij} = \frac{2\tilde{n}_i}{\tilde{n}_i + \tilde{n}_j} \quad (2-3)$$

$$r_{ij} = \frac{\tilde{n}_i - \tilde{n}_j}{\tilde{n}_i + \tilde{n}_j} \quad (2-4)$$

In most of cases, the substrate, layer 3, is high reflective, for example, metal reflects more than 99.5% at 1 THz [1]. It is reasonable to model  $r_{23} = -1$ .

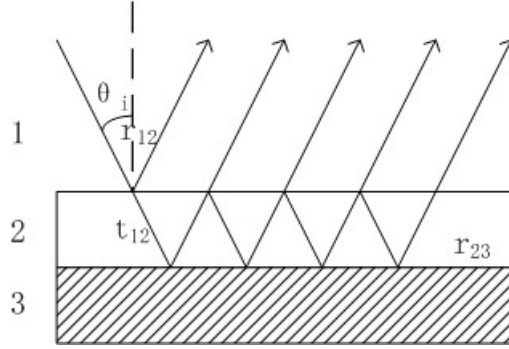


Figure 2. 1 Schematic representation of a light ray incident at a single layer coating

In practice, the length of time window is known; it is impossible to measure all the reflected waves. The number of reflected waves can be estimate as  $a$ .

The speed of light in the optical media is

$$v = \frac{c}{n} \quad (2-5)$$

And the time for one reflective wave needed is

$$\Delta t = \frac{2dn}{c} \quad (2-6)$$

Therefore, based on the time window, we can know how many reflective waves we can obtain in the time window roughly.

Then the transfer function is:

$$T_0(\omega) = r_{12} + \frac{t_{12} \cdot r_{23} \cdot t_{21} \cdot e^{-i2\beta_2} \cdot [1 - (r_{21} \cdot r_{23} \cdot e^{-i2\beta})^a]}{1 - t_{12} \cdot r_{23} \cdot t_{21} \cdot e^{-i2\beta_2}} \quad (2-7)$$

Where,  $a$  is the number of waves in the time window.

With films thin enough, the number of reflected waves  $a \rightarrow \infty$ , then the transfer function becomes



$$T_0(\omega) = r_{12} + \frac{t_{12} \cdot r_{23} \cdot t_{21} \cdot e^{-i2\beta_2}}{1 - t_{12} \cdot r_{23} \cdot t_{21} \cdot e^{-i2\beta_2}} \quad (2-8)$$

However, in practical, we usually measure the reflection wave from bare substrate as reference rather than the incident wave. The phase of reflection wave is different from the incident wave, which gives rise to a phase shifting consideration.

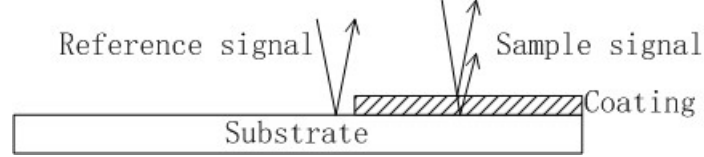


Figure 2. 2 A light ray incident at a single layer coating

Thus, the transfer function becomes:

$$T(\omega) = \frac{e^{i \cdot 2 \cdot \beta_1}}{r_{13}} \cdot T_0(\omega) \quad (2-9)$$

Where,

$\beta_1 = \omega n_1 d_2 / c$  is the phase shift accumulated.

In the transfer function, the refractive index and thickness of the layer,  $\tilde{n}_2$  and  $d_2$ , are unknown. If we have the measurement of the reflected electric field  $E_r$  and the incident electric field  $E_{r,0}$ , we can obtain  $T(\omega)$ . With the model, we can fit the measurement curves to obtain the unknown parameters.

## 2.2 Double-Layer Model

For two-layer modelling, the idea [19] is to replace the Fresnel reflection coefficient with the complete transfer function of the adjacent layer  $l$ .

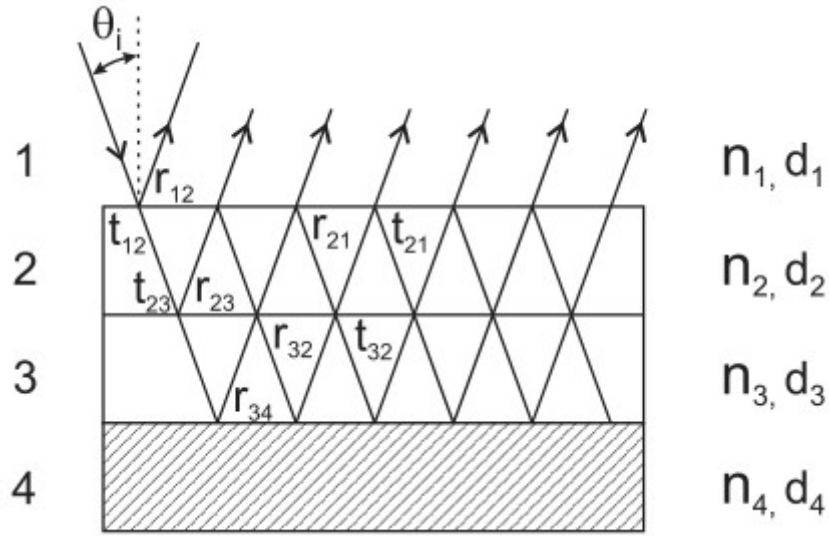


Figure 2. 3 Schematic representation of a light ray incident at a double-layer coating

If we let  $l$  denote the layer index, the transfer function is:

$$T_l(\omega) = r_{l-1,l} + \frac{t_{l-1,l} \cdot r_{l,l+1} \cdot t_{l,l-1} \cdot e^{-i2\beta_l}}{1 - t_{l-1,l} \cdot r_{l,l+1} \cdot t_{l,l-1} \cdot e^{-i2\beta_l}} \quad (2-10)$$

Now, we interpret the overlying layer  $l - 1$  again as a single layer with the simple transfer function like the previous layer  $l$ .

$$T_{l-1}(\omega) = r_{l-2,l-1} + \frac{t_{l-2,l-1} \cdot r_{l-1,l} \cdot t_{l-1,l-2} \cdot e^{-i2\beta_{l-1}}}{1 - t_{l-2,l-1} \cdot r_{l-1,l} \cdot t_{l-1,l-2} \cdot e^{-i2\beta_{l-1}}} \quad (2-11)$$

Therefore, we integrate the entire effects together and provide a full description of the multi-layer structure.

$$T_{total}(\omega) = r_{l-2,l-1} + \frac{t_{l-2,l-1} \cdot T_l(\omega) \cdot t_{l-1,l-2} \cdot e^{-i2\beta_{l-1}}}{1 - t_{l-2,l-1} \cdot T_l(\omega) \cdot t_{l-1,l-2} \cdot e^{-i2\beta_{l-1}}} \quad (2-12)$$

In the transfer function, the refractive indexes and thicknesses of the layers are unknown. We can use terahertz time-domain spectrometer to measure the time-domain reflective wave and get the reflected electric field  $E_r$  and the incident electric field  $E_{r,0}$  by Fourier transform. With the model of  $T_{total}(\omega)$ , we can fit the measurement curves to obtain the unknown parameters.

## 2.3 Incident Angle

When incident angle is considered, the incident angle  $\theta$  is measured, and the angle  $\beta$  can be estimated by Snell's law [27] for transparent materials.

$$\beta = \arcsin\left(\frac{n_i \sin \theta}{n_j}\right) \quad (2-13)$$

The Fresnel equations at an interface are:

$$t_{ij} = \frac{2\tilde{n}_i \cos \theta}{\tilde{n}_i \cos \beta + \tilde{n}_j \cos \theta} \quad (2-14)$$

$$r_{ij} = \frac{\tilde{n}_i \cos \beta - \tilde{n}_j \cos \theta}{\tilde{n}_i \cos \beta + \tilde{n}_j \cos \theta} \quad (2-15)$$

Through fitting we can calculate the ray length in the material, but the thickness of the layer is:

$$d = l \cdot \cos \beta \quad (2-16)$$

## 2.4 Model Complex Refractive Index

The refractive index  $n$  is complex and frequency independent. It has a relationship with the dielectric constants of the specific material.

$$n(\omega) = \sqrt{\epsilon(\omega)} \quad (2-17)$$

For different materials, an appropriate model for dielectric constants is chosen. For some cases, Drude–Lorentz model [23] is used.

$$\epsilon(\omega) = \epsilon_\infty + \frac{\omega_p^2}{\omega_0^2 - \omega^2 - i\gamma\omega} \quad (2-18)$$

Where,

$\epsilon_\infty$  is the high frequency limit of  $\epsilon(\omega)$ ;

$\omega_p$  is the plasma frequency;

$\omega_0$  is the characteristic frequency;

$\gamma$  is the relaxation rate of excitation.

For some other materials, especially liquid, Debye model [28] is usually used.

$$\epsilon(\omega) = \epsilon_{\infty} + \frac{\epsilon_s - \epsilon_{\infty}}{1 + i \cdot \omega \cdot \tau} \quad (2-19)$$

Where,

$\epsilon_{\infty}$  is the high frequency limit of  $\epsilon(\omega)$ ;

$\epsilon_s$  is the static dielectric constant;

$\tau$  is the characteristic time constant.

Therefore, the parameters  $\epsilon_{\infty}$ ,  $\omega_p$ ,  $\omega_0$ ,  $\gamma$  or  $\epsilon_{\infty}$ ,  $\epsilon_s$ ,  $\tau$  in the transfer function are to be find through fitting.

## 2.5 Differential Evolution (DE) Algorithm

For the least-squares fitting, there are many algorithms. Differential evolution (DE) algorithm [29] converges fast. I adopt this algorithm to fit the curve.

Differential Evolution (DE) does a parallel direct search by using parameter vectors. The dimension of the parameter vector is the number of parameter to fit. People choose a population number for the vectors. The initial vector population is generated randomly covering the whole estimated parameter range. Then we do mutations by adding a weighted difference between two vectors to a third vector. The parameters in the mutated vector are then mixed with another vector, target vector, to get a trial vector. After that we compare the parameters in the target vector and the trial vector, and then select the one who gives lower error to the final function to be in the next generation. This is called evolution. We keep this iteration until the final error fulfill the requirement.

## 2.6 Considerations About Substrate Water

When we measured the layer of oil on water, oil is not evenly distributed on the water surface, i.e. the thickness of the oil film varies. Furthermore, the level of water surface changes when oil is added in. Thus, the phase shift accumulated in Equation (2-9) would change. However, the ray length changed is difficult to measure. We set it as another parameter to fit. In other words, the ray length in the transfer function

$$T(\omega) = \frac{e^{i \cdot 2 \cdot \beta_1}}{r_{13}} \cdot T_0(\omega) \quad (2-20)$$

Where,

$\beta_1 = \omega n_1 d_{level} / c$  is the phase shift accumulated;

$d_{level}$  is related to the change of water surface position, which is another unknown parameter for fitting.

The parameters of water dielectric constants and refractive index applied in this essay are found in literature [30] .

$$\epsilon_{water}(\omega) = \epsilon_{\infty} + \frac{\epsilon_s - \epsilon_1}{1 + i\omega\tau_D} + \frac{\epsilon_1 - \epsilon_{\infty}}{1 + i\omega\tau_2} + \frac{A}{\omega_T^2 - \omega^2 + i\omega\gamma} \quad (2-21)$$

Where,

$$\tau_D = 9.36 \text{ ps}$$

$$\epsilon_s = 80.2$$

$$\epsilon_{\infty} = 2.5$$

$$\omega_T = 5.6 \text{ THz}$$

$$\frac{\gamma}{2\pi} = 5.9 \text{ THz}$$

$$A = 38 \text{ THz}^2$$

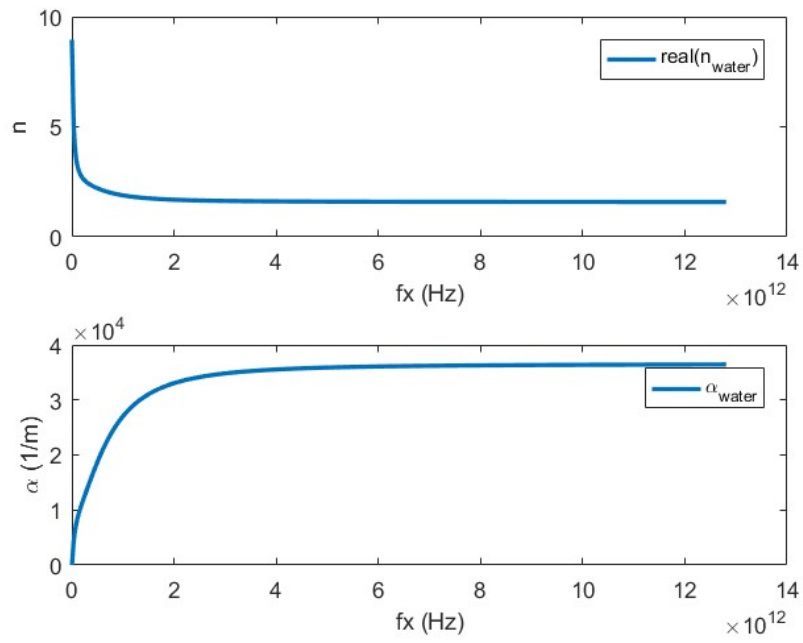


Figure 2. 4 The refractive index and absorption coefficient of water

## Chapter 3 Simulation

Before doing the experiments, simulations were applied to test and modify the algorithm. The algorithm was optimized for situations of applications. We first measured a reference terahertz signal with Picometrix T-Ray 2000 terahertz spectroscopy system in our laboratory. And then we model the specimen with known materials to calculate the theoretical transfer function. Through the theoretical transfer function, we calculated the theoretical reflected terahertz signal. Next, we added a noise on the theoretical reflected terahertz signal, modelling it as measured reflected terahertz signal. Therefore, with reference terahertz signal and measured reflected terahertz signal, we tested the algorithm by simulations.

### 3.1 Single-Layer Model

We measured the incident terahertz wave as the reference signal.

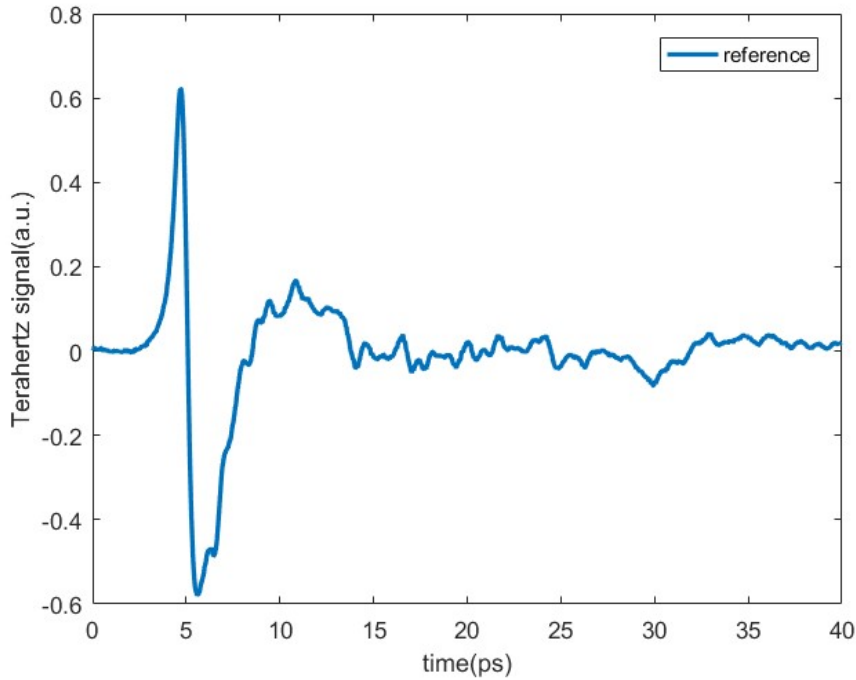


Figure 3. 1 Reference Signal

Firstly, we modelled the sample as a steel plate with a coating of ZnO. We used Drude–Lorentz model and modelled the material as ZnO, whose dielectric constants were found in the literature [31].

$$\epsilon(\omega) = \epsilon_{\infty} + \frac{\omega_p^2}{\omega_0^2 - \omega^2 - i\gamma\omega} \quad (3-1)$$

Where,

$$\epsilon_{\infty} = 4$$

$$\omega_p = 2\pi \cdot 25 \text{ THz}$$

$$\omega_0 = 2\pi \cdot 12 \text{ THz}$$

$$\gamma = 2\pi \cdot 1 \text{ THz}$$

$$d_2 = 600 \text{ } \mu\text{m}$$

The refractive index and absorption coefficient are shown in the following figures.

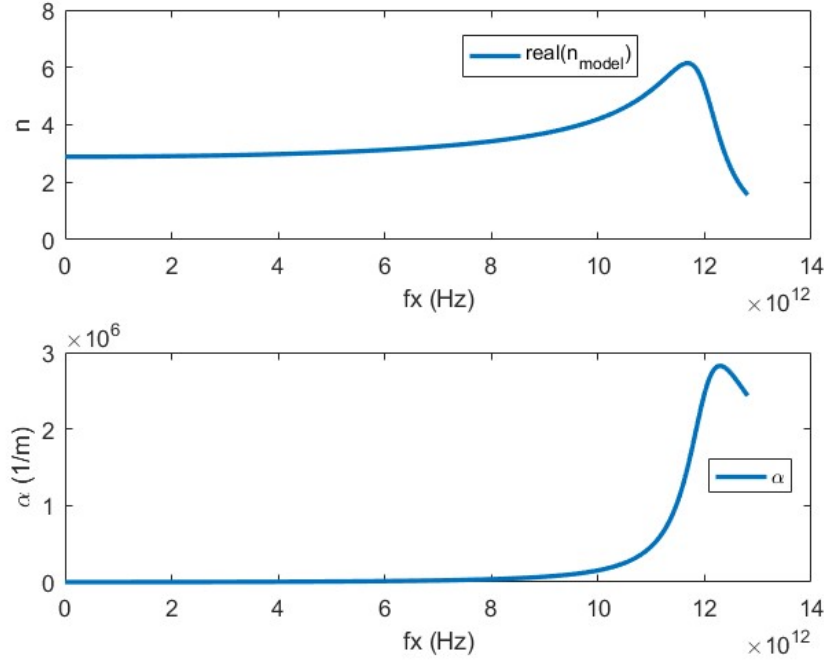


Figure 3. 2 Refraction Index and Absorption Coefficient of ZnO

From the results we can see that the refractive index is about 2.9 under 3 THz. We use the data to estimate that there would be 3 reflected waves in our time window, 40 ps.



Therefore, we can calculate the transfer function, the magnitude of the transfer function is shown in the following figure.

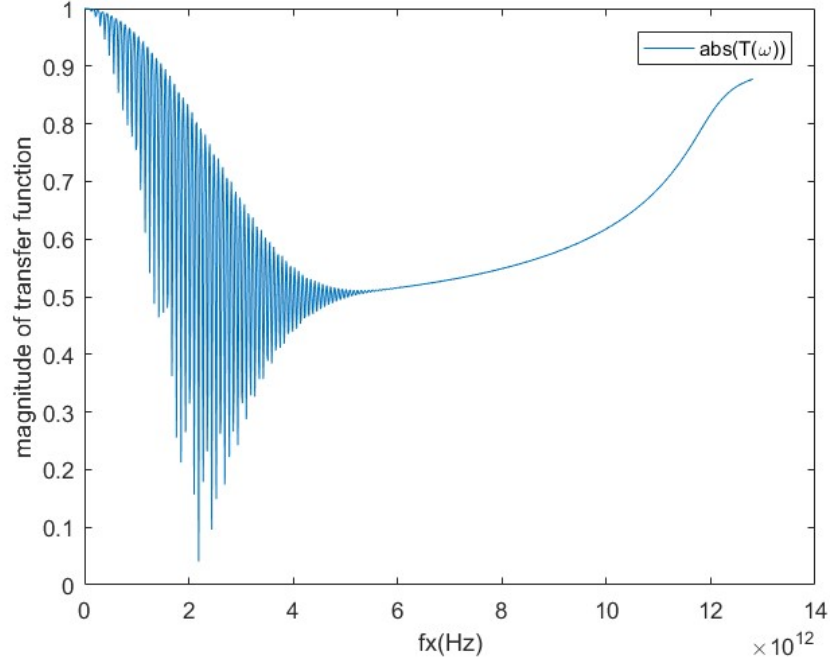


Figure 3. 3 Magnitude of The Transfer Function

After that, we can calculate the theoretical measured signal base on our model, as it shown in the following figure. There are three reflective measured in the time window, which is accordance with our expectation. And the time intervals between successive reflections also reflect the thickness of the coating layer.

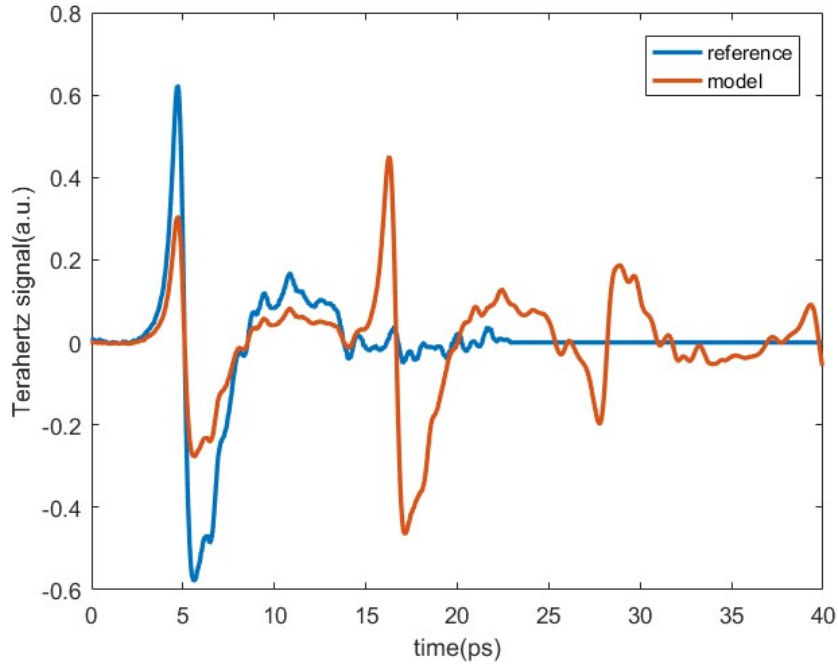


Figure 3. 4 Reference Signal and Modelled Signal in Time Domain

Then we simulated the measured signal by adding a white Gaussian noise on the model signal, and the signal-to-noise ratio (SNR) was 50 dB.

Having the reference and sample signals, there are five parameters in the transfer function to be find through fitting:  $\epsilon_{\infty}$ ,  $\omega_p$ ,  $\omega_0$ ,  $\gamma$ ,  $d_2$ . We adopted DE algorithm to fit the measured curve and fit the measured curve with the least-squares of error between the fitting curve with the measured curve. As it shown in the following figure, the curve of time-domain signal fits well.

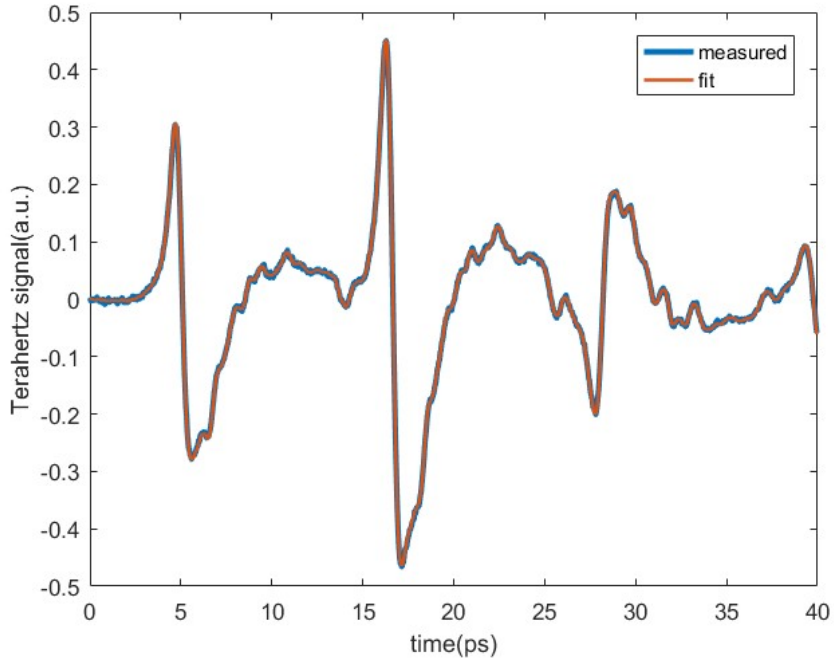


Figure 3. 5 Fitted Time-Domain Signal

Finally, after iterations the group of the fitting results are shown in the following table.

Table 3. 1 Parameters comparison of fitting

Variable	Fit	Model
$\epsilon_{\infty}$	4.0039	4
$\omega_p$ (THz)	158.06	157.08
$\omega_0$ (THz)	73.383	75.398
$\gamma$ (THz)	7.9729	6.2832
$d$ ( $\mu\text{m}$ )	589.32	600

Because in DE algorithm, the fitting parameters are generated randomly under the limitations, the results are different every time. The thickness we finally obtained is accurate, the error is 1.8%. The results of dielectric constants are also reasonable.

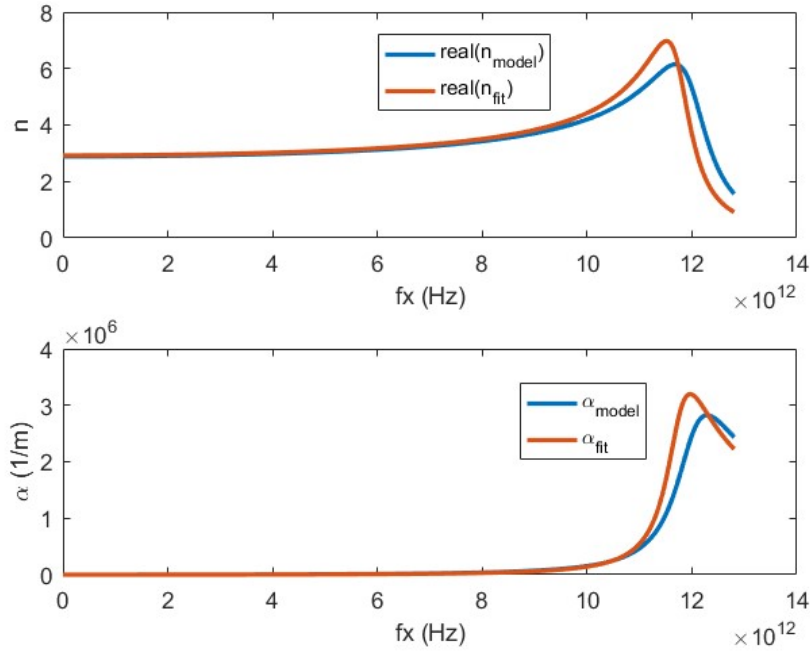


Figure 3. 6 Fitting results of refractive index and absorption coefficient

The curve fitting and parameters calculation show a good result for the method.

### 3.2 Double-Layer Model

We also tested the algorithm for two-layer materials on a metal substrate. The sample is modelled as a steel plate with a layer of ZnO coating on it and another layer of CS<sub>2</sub> on the top of ZnO coating.

We modelled the first layer as CS<sub>2</sub>, using Debye model. The dielectric constants [28] are set to the model.

$$\epsilon(\omega) = \epsilon_{\infty,1} + \frac{\epsilon_{s,1} - \epsilon_{\infty,1}}{1 + i \cdot \omega \cdot \tau_1} \quad (3-2)$$

Where,

$$\epsilon_{\infty,1} = 2.511$$

$$\epsilon_{s,1} = 2.62$$

$$\tau_1 = 600 \text{ fs}$$

$$d_1 = 900 \text{ } \mu\text{m}$$

We modelled the second layer as ZnO with Drude–Lorentz model. The dielectric constants were found in literature [31], and set as follows.

$$\epsilon(\omega) = \epsilon_{\infty,2} + \frac{\omega_{p,2}^2}{\omega_{0,2}^2 - \omega^2 - i\gamma_2\omega} \quad (3-3)$$

Where,

$$\epsilon_{\infty,2} = 4$$

$$\omega_{p,2} = 2\pi \cdot 25 \text{ THz}$$

$$\omega_{0,2} = 2\pi \cdot 12 \text{ THz}$$

$$\gamma_2 = 2\pi \cdot 1 \text{ THz}$$

$$d_2 = 900 \text{ } \mu\text{m}$$

The dielectric constants, and the complex refractive index are calculated.

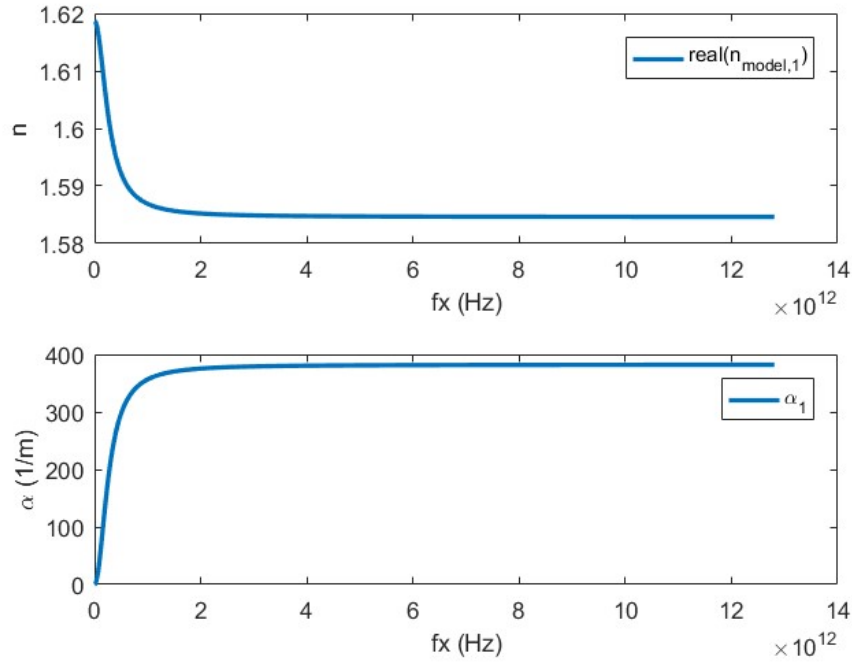


Figure 3. 7 Refractive index and absorption coefficient of layer 1

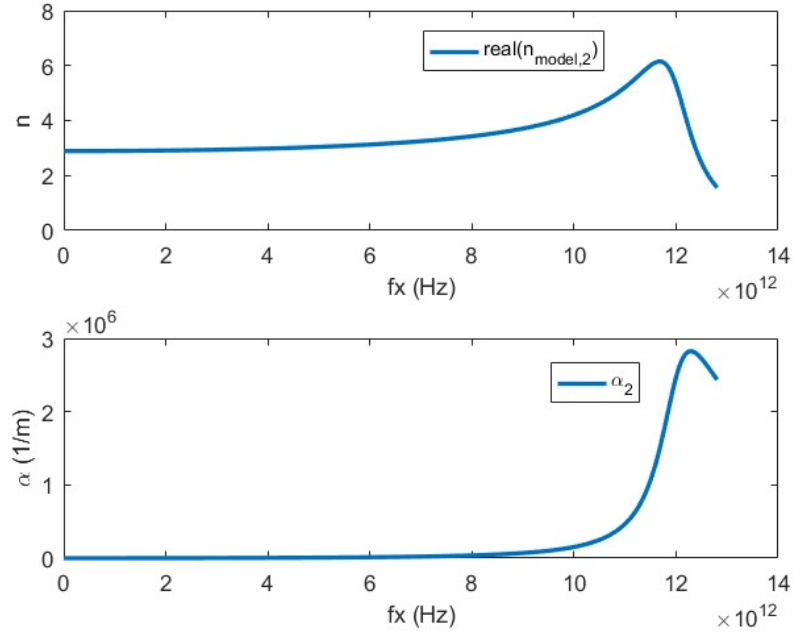


Figure 3. 8 Refractive index and absorption coefficient of layer 2

After that, we can calculate the transfer function and the theoretical measured signal base on our double-layer model.

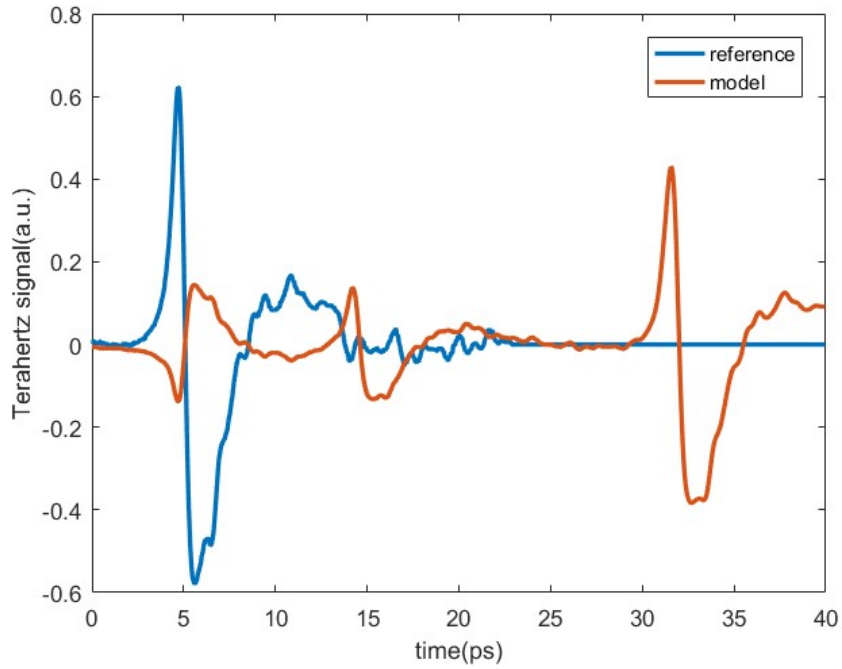


Figure 3. 9 Reference signal and modelled signal in time domain

Then we simulated the measured signal by adding a white Gaussian noise on the model signal, and the signal-to-noise ratio (SNR) was 50 dB.

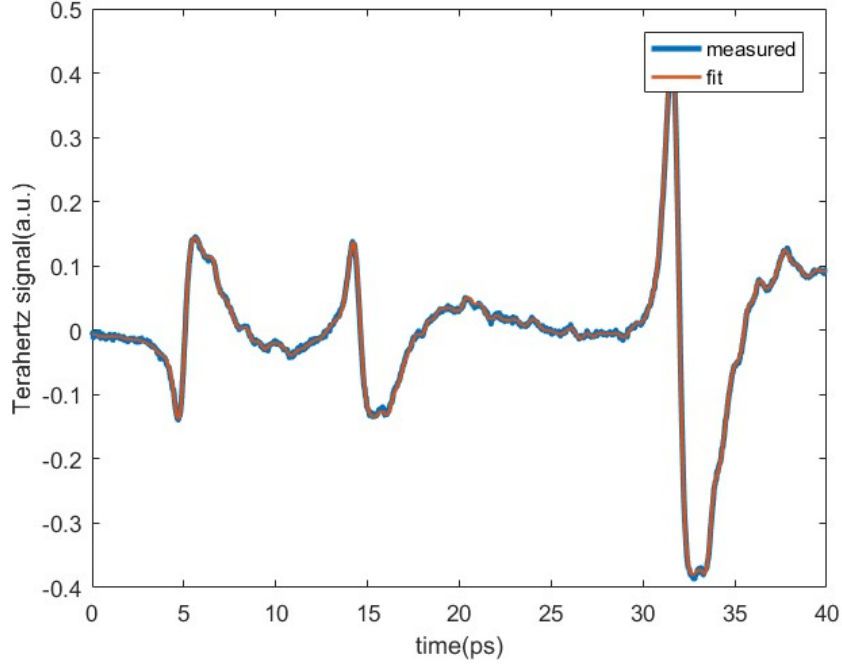


Figure 3. 10 Fitted time-domain signal

Finally, one group of the fitting results are:

Table 3. 2 fitting results for the layers

Layer 1			Layer 2		
Variable	Fit	Model	Variable	Fit	Model
$\epsilon_{\infty}$	2.4652	2.511	$\epsilon_{\infty}$	3.6870	4
$\epsilon_s$	2.5782	2.62	$\omega_p$ (THz)	155.97	157.08
$\tau$ (fs)	600.35	600	$\omega_0$ (THz)	73.273	75.398
$d$ ( $\mu m$ )	906.75	900	$\gamma$ (THz)	3.3362	6.2832
			$d$ ( $\mu m$ )	907.22	900

The error of thickness is 0.8%.

The error of the thickness measurement of double-layer model looks less than signal-layer model. However, it doesn't mean that more layers make less error. Many times of test and many groups of results we got in the simulation show that the error varies with the random noise and the random search in DE algorithm.

### 3.3 Phase Shift

In practical situations we usually measure the reflection from bare substrate as reference. Thus, considering the phase shifting, the phase of the first reflective wave in the sampled time-domain signal leads the reference signal.

The theoretical reflected terahertz signal was calculated and shown in the following figure when the reference signal was considered as the reflection by the bare steel plate substrate. The first reflective wave by the surface of first layer leads the reference signal as we expected. And the time intervals of the reflective waves reflects the thickness of the coating layer.

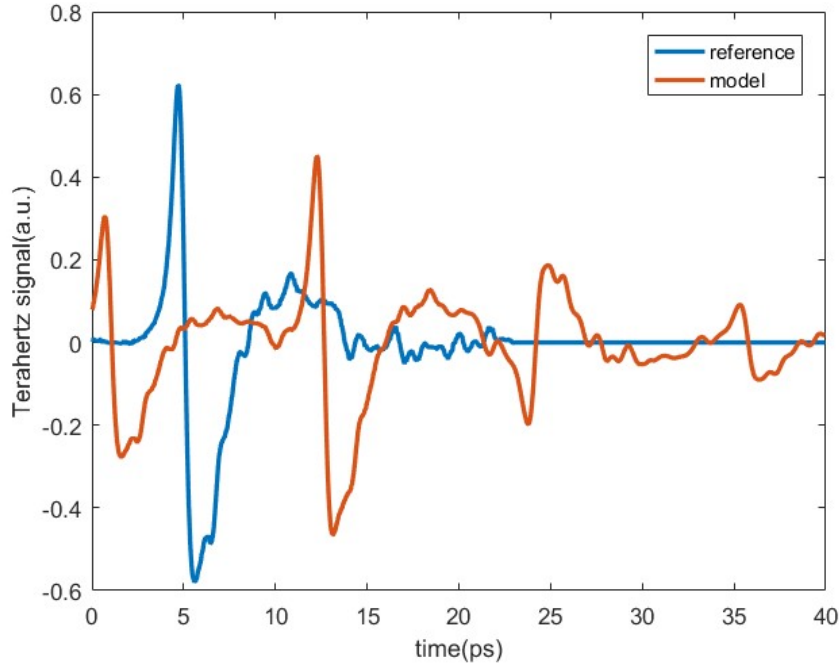


Figure 3. 11 reference signal and modelled signal in time domain

The transfer function changes, but the fitting parameters are the same. The fitting results are shown in the following table.

Table 3. 3 Fitting Results Comparison

Variable	Fit	Model
$\epsilon_{\infty}$	4.5262	4
$\omega_p$ (THz)	157.25	157.08



$\omega_0$ (THz)	77.608	75.398
$\gamma$ (THz)	4.6749	6.2832
$d$ ( $\mu m$ )	589.73	600

Because in DE algorithm, the fitting parameters are generated randomly under the limitations, the results are different every time. The thickness we finally obtained looks accurate, the error is 1.8%. And the results are accordance with the premier tests.

### 3.4 Analysis

Through the simulations, we tested and modify the algorithm. The agreement of the results confirms the development of the method.

From the mathematical perspective, however, if Drude-Lorentz model is adopted to describe the dielectric constant of the material, it is very important to have pre-knowledge of the material parameters, in other words, to have relatively accurate initial values. We did several experiments and analysis to this problem.

For unknow materials measurement, the initial value can be measured with other methods. For example, we tried to measure the dielectric parameters with transmission terahertz time-domain spectroscopy. However, the bandwidth of the spectrometer is limited. For example, the material ZnO has a powerful absorption at frequency 12.42 THz due to transverse optical phonon resonance [31], which lies out of the bandwidth of our terahertz time-domain spectrometer. Thus, it is unlikely to measure this parameter accurately in Drude-Lorentz model with this method. People can use other analysis to get the material parameters before applying this thickness measurement, but it is out of the topic in this research.

On the other hand, Debye model gives good results both in parameter measurement with transmission spectroscopy and thickness measurement with reflection spectroscopy due to the less number of unknown parameters in the model. Furthermore, DE algorithm allows fast convergence searching for solutions in a large range. The fitting range of the parameters can be set large enough for vast area of materials. This method would give results about the material parameters and the thickness of the coating together. Besides,

in most cases, Debye model gives accurate theoretical prediction for dielectric constants. For example, liquid specimen is well described by Debye model.

Therefore, through the simulations, tests, and analysis, we conclude that this algorithm works well for measurement of thickness for unknown materials, based on which we designed and performed experiments.

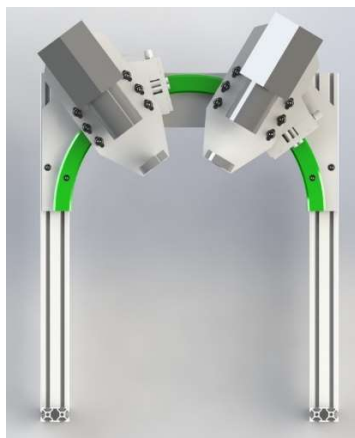
## Chapter 4 Experimental work

Having this method, we measured the thickness of a sticker on a steel plate. This method calls for accurate phase measurement, the original experimental setup is not suitable because it is very difficult to ensure the measuring conditions same between reference signal and specimen signal measurements. Therefore, we designed a new experimental setup. This setup can broaden the application range, for example, it allows measurement of liquid. We also measure the thickness of oil film on water surface, and the phase shifting fitting method becomes important.

### 4.1 Experimental setup

T-Ray 2000, a product of Picometrix Inc., was applied for the experiments. This system is a compact, fiber-pigtailed terahertz spectroscopy system for commercial use. The heart of the system consists of two fiber-pigtailed hermetically sealed transmitter and receiver. Optical fibers and electronics accessories attach the cases to a control box, containing the computer-controlled optical delay and other monitors. Controlling the system and data taking is accomplished by a computer software.

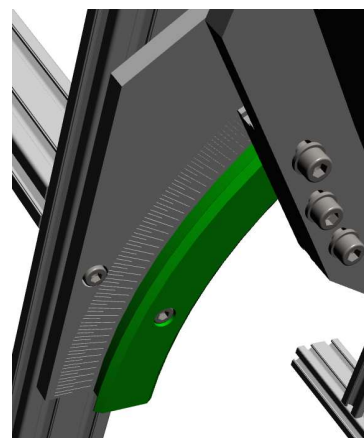
We designed and manufactured a stage. It allows transmission and reflection mode spectroscopy. The terahertz transmitter and receiver are mounted on sliders respectively, and their positions are adjusted on a semicircular guide. The height of the stage can be adjusted, and there are scales on the plane through which the angle can be read.



( a )



( b )



( c )

Figure 4. 1 ( a ) Front view; ( b ) Axonometric; ( c ) Detail image of the scales

The size and dimension of the parts and the distances of the lenses are customized for the transmitter and receiver. The optical path is carefully designed. The focus of the lenses falls at the center of the guide's circle, and slotted holes are designed for fine tuning.

This experimental setup could help us with accurate positioning between the sample and reference more conveniently, and it allows measurement of liquid specimen.

## 4.2 Reflective Measurement

### 4.2.1 Stickers on steel plate

Having this experimental setup, we measured the thickness of a sticker on a steel plate. The reflected terahertz wave by bare steel plate is the reference signal, while the specimen signal is reflected by the sticker area. The time-domain terahertz signals were measured by T-Ray 2000 terahertz spectroscopy system.

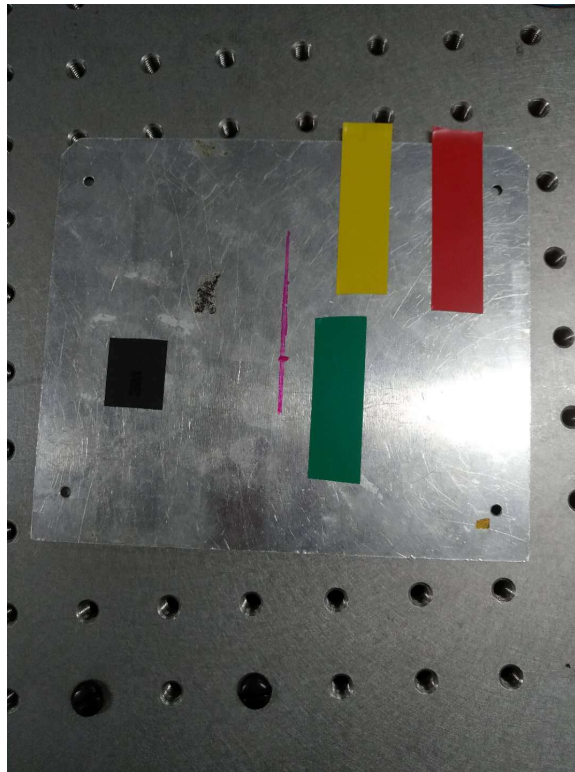


Figure 4. 2 Four stickers on a steel plate

The time-domain terahertz waves are shown in the following figures.

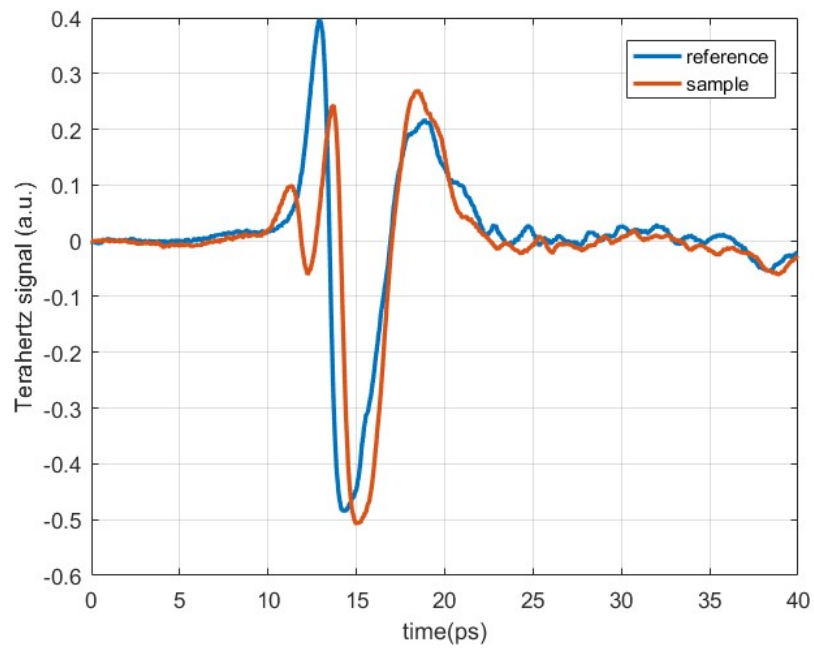


Figure 4. 3 Terahertz signal of yellow sticker in time domain

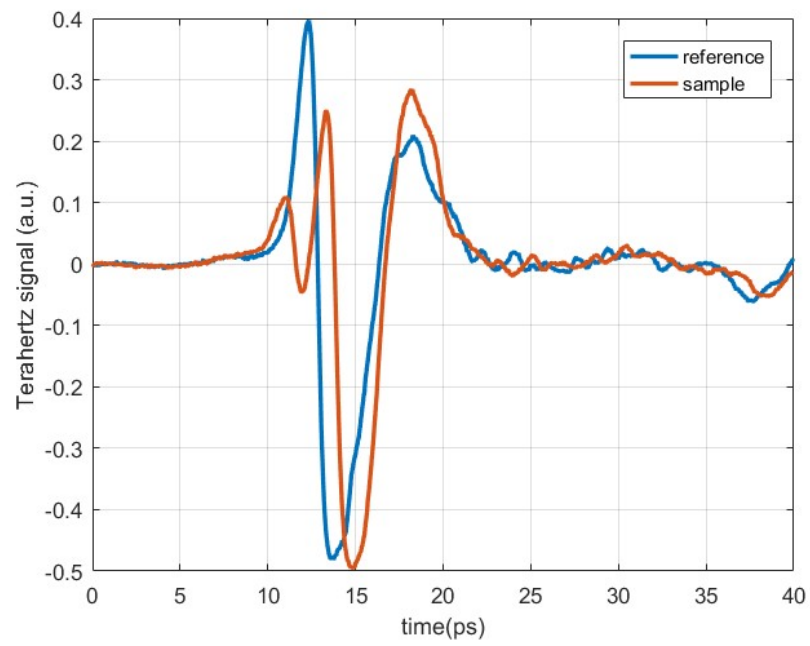


Figure 4. 4 Terahertz signal of red sticker in time domain

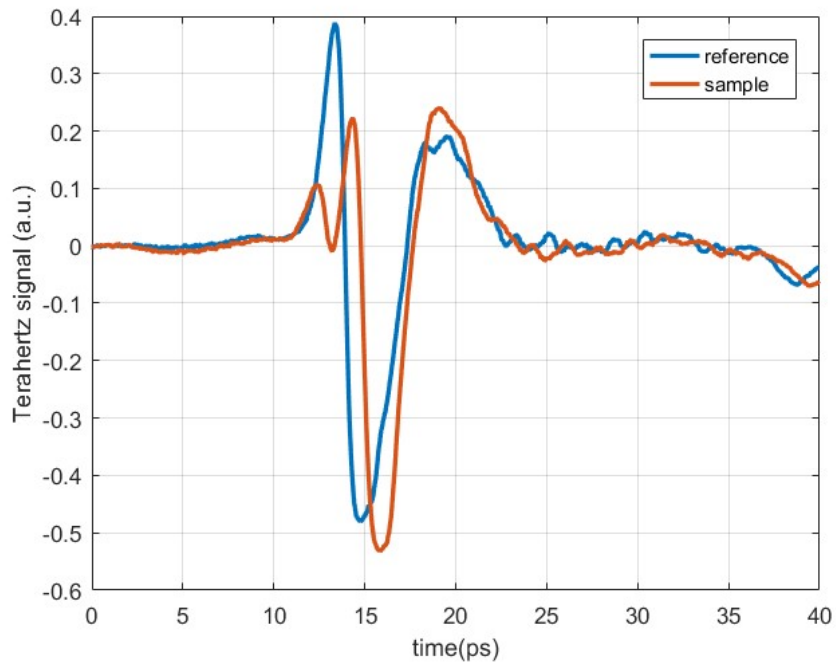


Figure 4. 5 Terahertz signal of black sticker in time domain

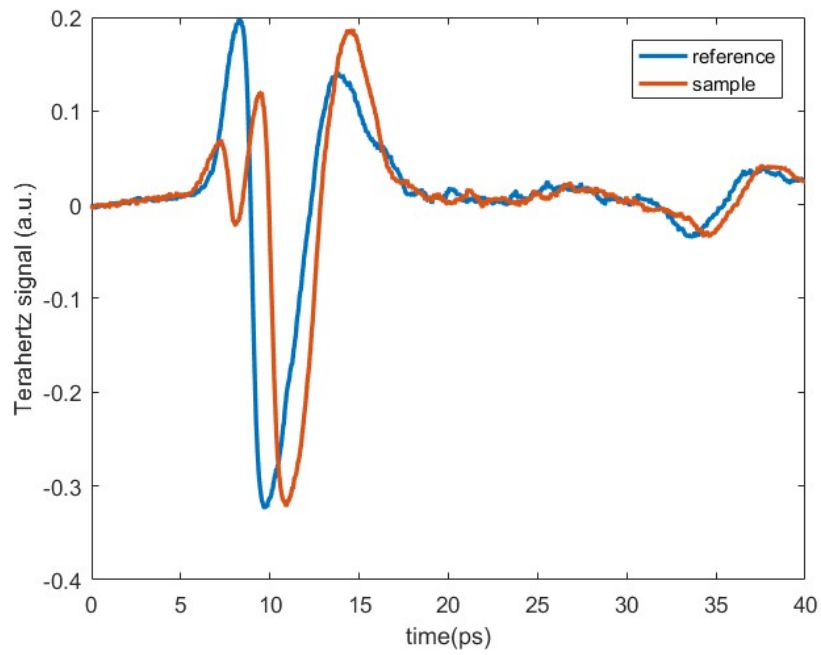


Figure 4. 6 Terahertz signal of green sticker in time domain

After fitting, we can obtain the results of thickness.

### 4.2.2 Oil on water

The reference signal is the reflected terahertz wave by the water surface. After reference signal measured, we added 1 mL oil on water surface with an injector. The inner diameter of the container is 64.6 mm; thus, the oil film would be about 305  $\mu\text{m}$  if it distributed evenly on the water surface. However, it can be observed that the oil isn't evenly distributed on the surface of water due to surface tension, and the distribution changes over time. It can also be observed in the time-domain terahertz waves measured at different times.

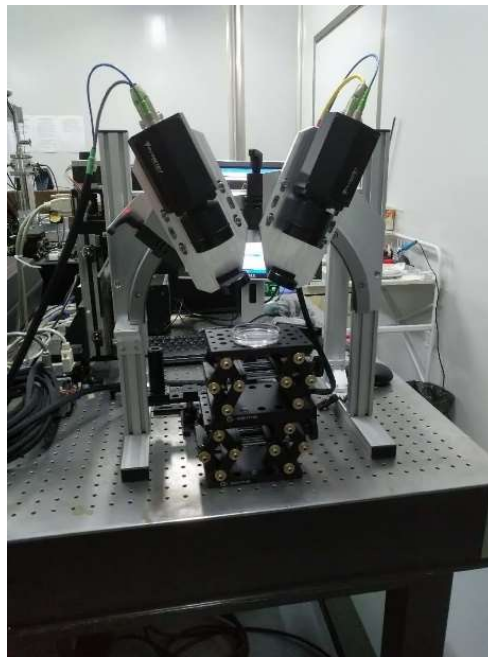


Figure 4. 7 Experimental Setup for Measurement of Oil on Water

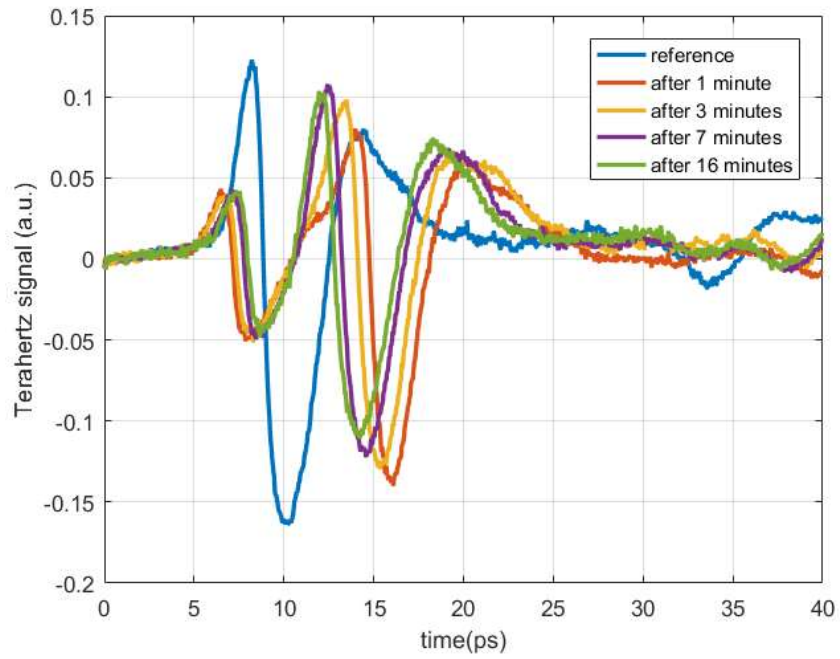


Figure 4. 8 Terahertz waves in time domain measured at different times

After fitting, the results of oil film thickness and the water level changes are obtained.



## Chapter 5 Results and discussion

### 5.1 Stickers on steel plate

Single-layer model is used for modelling the layer, and Debye model is used for modelling the refractive index. After fitting we get the fitting results of the time-domain terahertz waves, they are shown in the following figures.

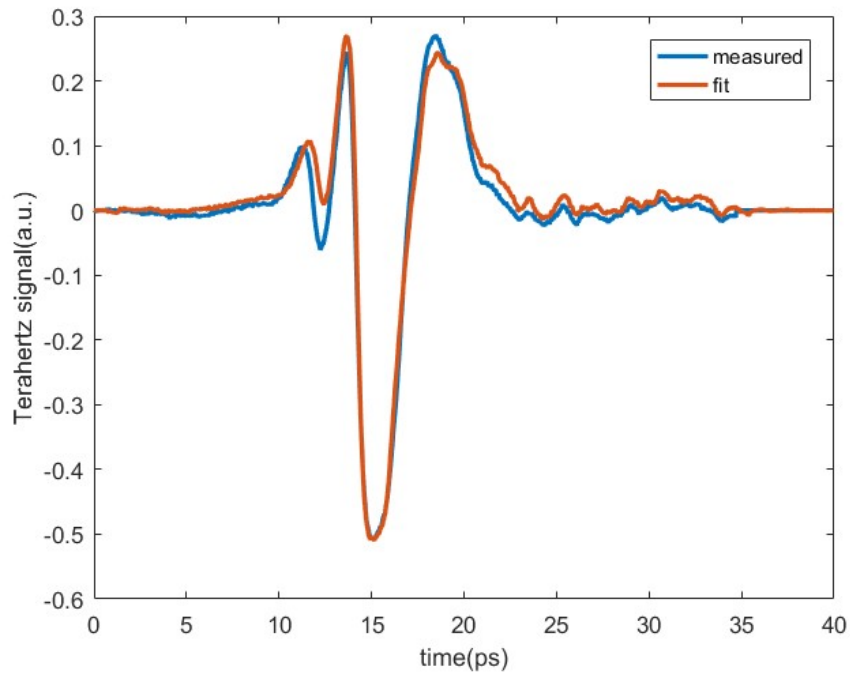


Figure 5. 1 Fitting results of time-domain wave of the yellow sticker

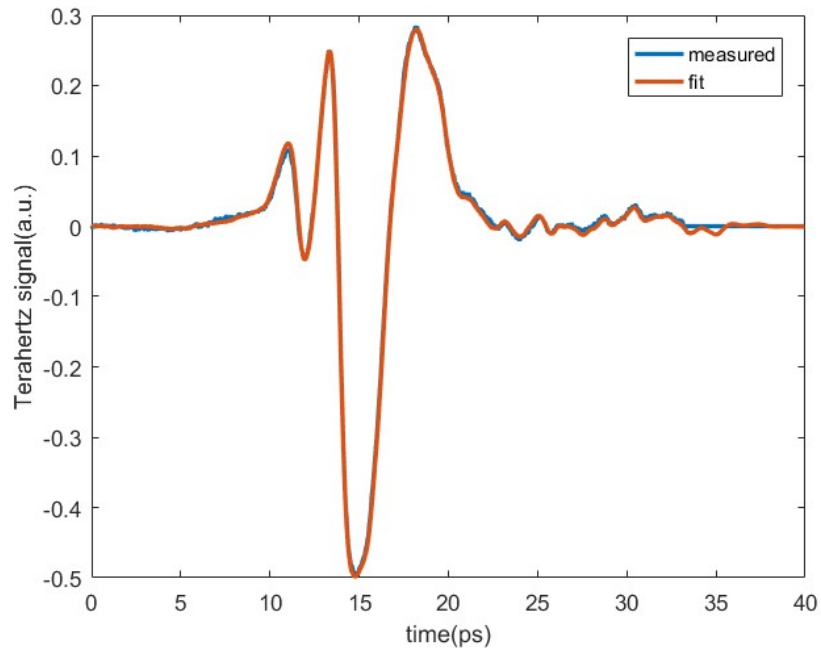


Figure 5. 2 Fitting results of time-domain wave of the red sticker

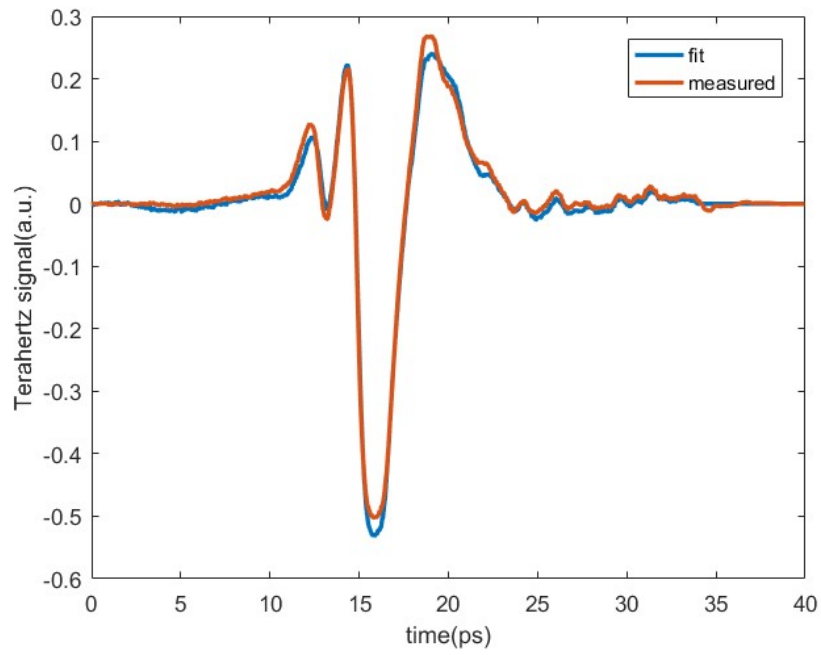


Figure 5. 3 Fitting results of time-domain wave of the black sticker

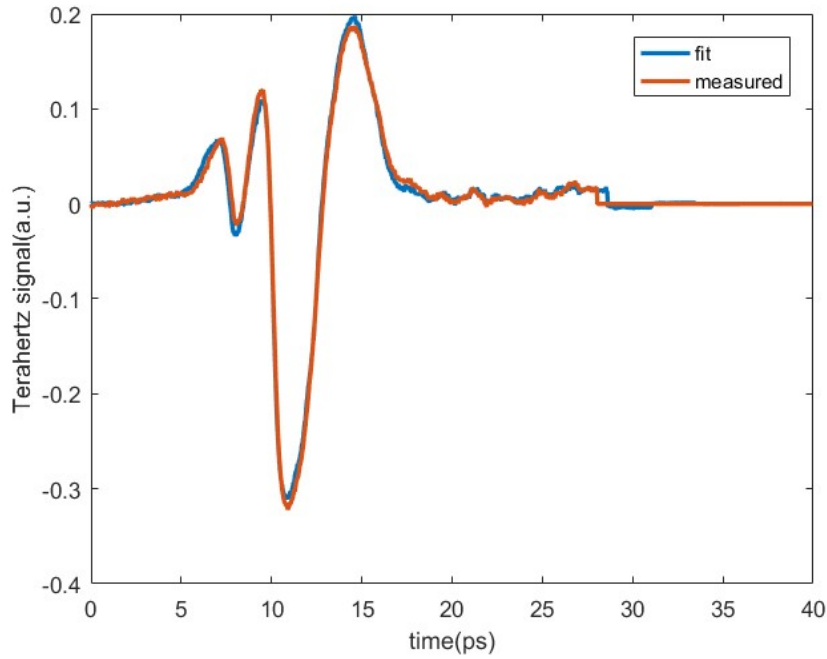


Figure 5. 4 Fitting results of time-domain wave of the black sticker

The experiment fitting results of the thickness are summarized in Table 5. 1.

Table 5. 1 Fitting Results of The Sticker

Sticker	Thickness measured by micrometer ( $\mu m$ )	Thickness measured by fitting ( $\mu m$ )	Error
Yellow	216	209.94	-2.8%
Red	208	202.81	-2.5%
Black	182	175.15	-3.8%
Green	198	204.64	3.4%

Compared with the thickness of the stickers measured by a micrometer, the errors of the thickness are no more than 4%. The stickers are not very hard; thus, when measured by a micrometer, the readings of the thickness would also give errors. Therefore, the measurement by our terahertz time-domain spectroscopy method is applicable. The fitting results would provide us a satisfactory fit of dielectric constants or refraction index, but the parameters may not have any physical meaning for mixtures like stickers. Nevertheless, the results provide references for further material analysis.

## 5.2 Oil on water

As for oil thickness on water surface, phase shifting caused by water surface level change has to be considered in the algorithm. Single-layer model is used for modelling the layer, and Debye model is used for modelling the refractive index. After fitting we get the fitting results of the time-domain terahertz waves, they are shown in the following figures.

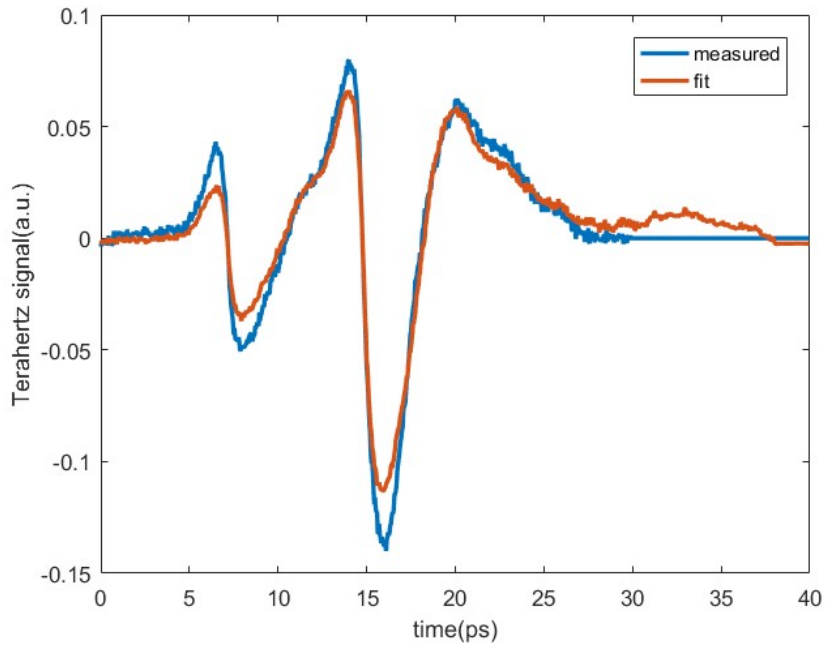


Figure 5. 5 Fitting results of time-domain wave measured after 1 minute

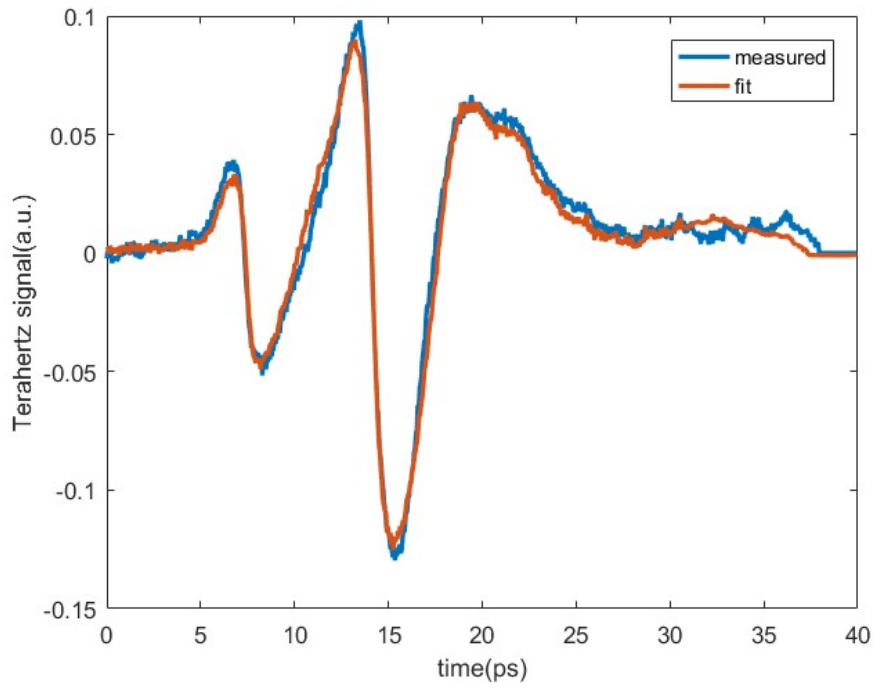


Figure 5. 6 Fitting results of time-domain wave measured after 3 minutes

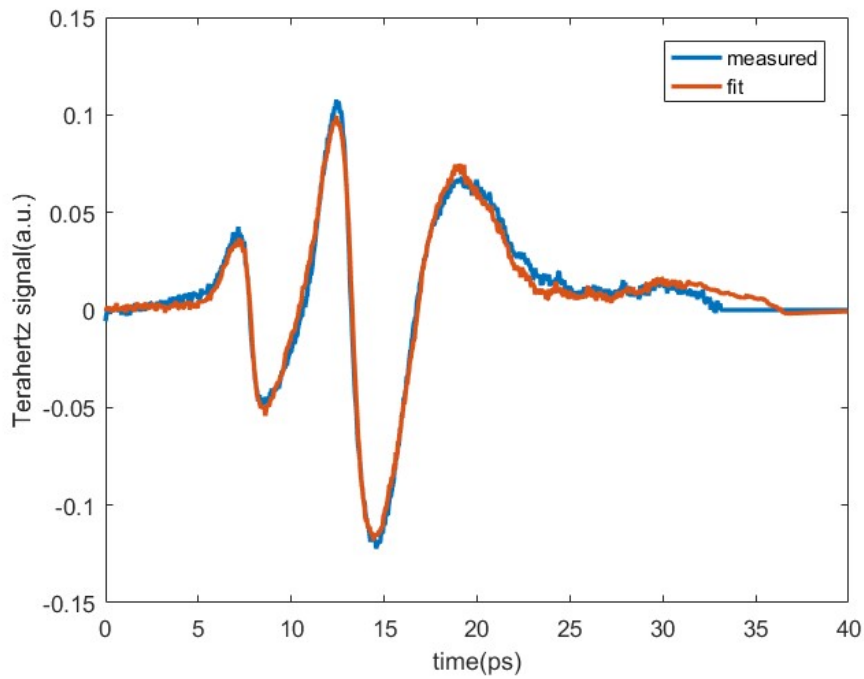


Figure 5. 7 Fitting results of time-domain wave measured after 7 minutes

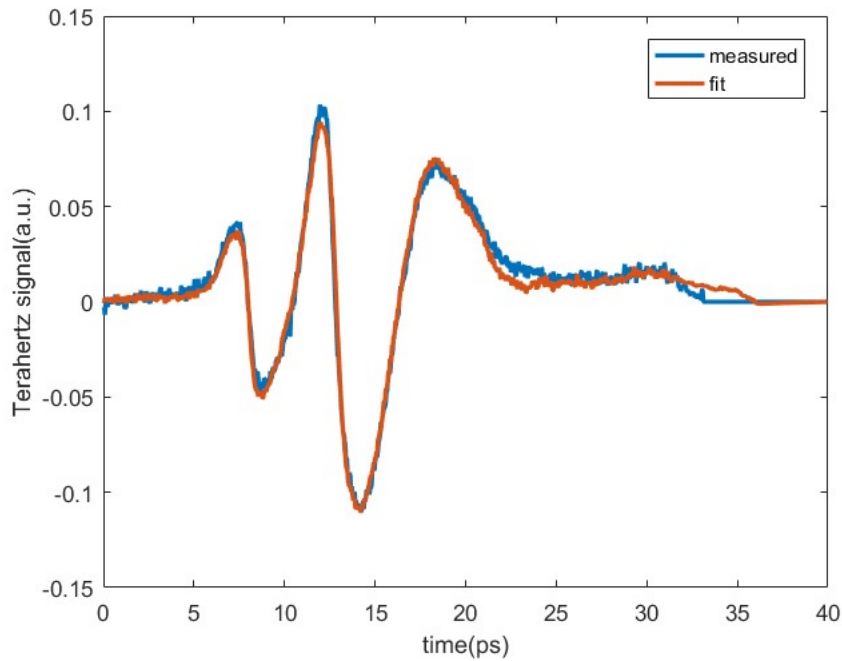


Figure 5. 8 Fitting results of time-domain wave measured after 16 minutes

The results of oil film thickness and the water level changes are shown in Table 5.

2. The change of water level reflects the difference between the water level when measuring the reference signal and sample signal.

Table 5. 2 Results of Thickness

Group	1	2	3	4
Thickness Fit ( $\mu m$ )	887	701	548	482
Change of Water level ( $\mu m$ )	236	198	135	105

As time goes on, the thickness of oil film becomes thinner and thinner, which reflects the fact that the oil spreads on the surface of water. Meanwhile, the change of water level becomes thinner, which is accordance to the physical principle of buoyancy. The volume of displaced fluid doesn't change, but as the oil spreads, the area increases, and the water level drops.

## Chapter 6 Conclusions and proposal for future work

This research confirms the previous findings and gives us a practical method for reflective terahertz spectroscopy. Additionally, the experimental setup extends the application area for terahertz spectroscopy. Besides, the consideration of phase shift about liquid substrate contributes to existing modelling knowledge.

As it illustrated in the simulation part, the results are accurate; therefore, the modelling and fitting method is applicable. When applying this method to the experimental work, we usually set the fitting parameters to cover most practical cases for unknown materials. DE algorithm allows fast convergence for searching results in a large range. The parameters may not have any physical meaning for mixtures; nevertheless, the results provide references for further material analysis.

The newly designed experimental setup provides opportunities for more applications. It not only makes it easier to measure coating on solid substrate, but also allows measurements for liquids. The experiments get good results. Moreover, this study also enhanced our understanding for liquid substrate. The problem of unknown phase shift caused by level change is solved. The algorithm innovatively introduces an unknown variable of the position of the liquid surface, making it possible to measure the thickness of oil contamination on the surface.

From this research we have developed a method for thickness measurement with reflective terahertz time-domain spectroscopy as well as a set of experimental setups. This study will serve as a base for future studies.

A number of new applications can be considered. First of all, real-time monitoring for oil pollution over vast area open water, like oceans, can be developed by the measurement of oil thickness on water surface. Besides, some improvement on the experimental setup can be developed. We can apply electric displacement platform and rotating platform to build 3D measurement setups. With more development on algorithm and system, terahertz spectroscopy imaging system can be built. We can also have more research about algorithm and other modelling methods, making the calculation faster and

more accuracy. In our common cases, Debye model is applied, while there are other models such as Gaussian, Fano, or Tauc–Lorentz. Analysis of the materials inspected in advance is needed according to the interactions with terahertz radiation.



## References

- [1] Y. S. Lee, *Principles of Terahertz Science and Technology*, New York: Springer Science+Business Media, LLC, 2009.
- [2] W. Zouaghi, M. D. Thomson, K. Rabia, R. Hahn, V. Blank and H. G. Roskos, "Broadband terahertz spectroscopy: principles, fundamental research and potential for industrial applications," *European Journal of Physics*, vol. 34, pp. S179-S199, 2013.
- [3] Z. Zhao and Y. Wang, "Development of a portable terahertz time- domain spectrometer," *Journal of Terahertz Science and Electronic Information Technology*, vol. 11, 2013.
- [4] J. V. Rudd, D. Zimdars and M. Warmuth, "Compact, fiber-pigtailed, terahertz imaging system," *Proceedings of SPIE*, vol. 3934, pp. 27-35, 2000.
- [5] N. Vieweg, N. Krumbholz, T. Hasek, R. Wilk, V. Bartels, C. Keseberg, V. Pethukov, M. Mikulics, L. Wetenkamp and M. Koch, "Fiber-coupled THz spectroscopy for monitoring polymeric compounding processes," *Proceedings of SPIE*, vol. 6616, 2007.
- [6] F. Ellrich, T. Weinland, D. Molter, J. Jonuscheit and R. Beigang, "Compact fiber-coupled terahertz spectroscopy system pumped at 800 nm wavelength," *Review of Scientific Instruments*, vol. 82, 2011.
- [7] B. Sartorius, H. Roehle, H. Künzel, J. Böttcher, M. Schlak, D. Stanze, H. Venghaus and M. Schell, "All-fiber terahertz time-domain spectrometer operating at 1.5  $\mu\text{m}$  telecom wavelengths," *Optics Express*, vol. 16, no. 13, pp. 9565-9570, 2008.
- [8] S.-P. Han, N. Kim, H. Ko, H.-C. Ryu, J.-W. Park, Y.-J. Yoon, J.-H. Shin, D. H. Lee, S.-H. Park, S.-H. Moon, S.-W. Choi, H. S. Chun and K. H. Park, "Compact fiber-pigtailed InGaAs photoconductive antenna module for terahertz-wave generation and detection," *Optics Express*, vol. 20, 2012.

- [9] S.-P. Han, H. Ko, N. Kim, H.-C. Ryu, C. W. Lee, Y. A. Leem, D. Lee, M. Y. Jeon, S. K. Noh, H. S. Chun and K. H. Park, “Optical fiber-coupled InGaAs-based terahertz time-domain spectroscopy system,” *Optics Letters*, vol. 36, 2022.
- [10] N. Vieweg, F. Rettich and A. Deninger, “Terahertz-time domain spectrometer with 90 dB peak dynamic range,” *Journal of Infrared Millimeter & Terahertz Waves*, vol. 35, pp. 823-832, 2014.
- [11] K. Merghem, S. F. Busch, F. Lelarge, M. Koch, A. Ramdane and J. C. Balzer, “Terahertz Time-Domain Spectroscopy System Driven by a Monolithic Semiconductor Laser,” *Infrared Milli Terahz Waves*, vol. 38, pp. 958-962, 2017.
- [12] “T-Ray 5000,” Picometrix, [Online]. Available: <http://advancedphotonix.com/thzsolutions/products/t-ray-5000/>. [Accessed 7 7 2016].
- [13] “TeraPulse 4000 – THz Pulsed Imaging and Spectroscopy,” TeraView, [Online]. Available: <http://www.teraview.com/products/TeraPulse%204000/index.html>. [Accessed 7 7 2016].
- [14] “Fiber Coupled Terahertz Spectrometer T-FIBER series,” Ekspla, [Online]. Available: <http://www.ekspla.com/product/fiber-couple-terahertz-spectrometer>. [Accessed 7 7 2016].
- [15] “TERA K15 All fiber-coupled Terahertz Spectrometer,” MenloSystems, [Online]. Available: <http://www.menlosystems.com/products/thz-time-domain-solutions/all-fiber-coupled-terahertz-spectrometer/>. [Accessed 7 7 2016].
- [16] “Time-Domain Spectroscopy Platform,” Toptica, [Online]. Available: [http://www.toptica.com/products/terahertz\\_generation/fs\\_packages/teraflash.html](http://www.toptica.com/products/terahertz_generation/fs_packages/teraflash.html). [Accessed 9 7 2016].
- [17] F. Ospald, W. Zouaghi, R. Beigang, C. Matheis, J. Jonuscheit, B. Recur, J.-P. Guillet, P. Mounaix, W. Vleugels, P. V. Bosom, L. V. González, I. López and R. M. Edo, “Aeronautics composite material inspection with a terahertz time-domain spectroscopy system,” *Optical Engineering*, vol. 53 (3) , 2014.

- [18] D. Zhao, J. Ren, X. Qao and L. Li, "Application of Terahertz Time-Domain Spectroscopy in Nondestructive Testing of Adhesion Quality," *Proceedings of SPIE*, vol. 9674, 2015.
- [19] S. Krimi, J. Klier, J. Jonuscheit, G. v. Freymann, R. Urbansky and . R. Beigang , "Highly accurate thickness measurement of multi-layered automotive paints using terahertz technology," *Applied Physics Letters*, vol. 109, 2016.
- [20] Irl N. Duling III, "Industrial Deployment of Time Domain Terahertz Systems," Picometrix, 2014.
- [21] T. Fukuchi, N. Fuse, M. Okada, T. Fujii, M. Mizuno and K. Fukunaga, "Measurement of Refractive Index and Thickness of Topcoat of Thermal Barrier Coating by Reflection Measurement of Terahertz Waves," *Electronics and Communications in Japan*, vol. 96, pp. 702-708, 2013.
- [22] M. Sudo, J. Takayanagi and H. Ohtake, "Nondestructive thickness measurement system for multiple layers of paint based on femtosecond fiber laser technologies," *Journal of Infrared Millimeter & Terahertz Waves*, 2016.
- [23] J. van Mechelen, A. Kuzmenko and H. Merbold, "Stratified dispersive model for material characterization using terahertz time-domain spectroscopy," *OPTICS LETTERS*, vol. 39, pp. 3853-3856, 2014.
- [24] K. Su, Y.-C. Shen and A. Zeitlet, "Terahertz Sensor for Non-Contact Thickness and Quality Measurement of Automobile Paints of Varying Complexity," *IEEE Transactions on Terahertz Science and Technology*, vol. 4, pp. 432-439, 2014.
- [25] S. P. Singh, A. K. Jha and M. J. Akhtar, "A Contactless Thickness Measurement of Multilayer Structure using Terahertz Time Domain Spectroscopy," in *IEEE Conference on Antenna Measurements & Applications*, 2015.
- [26] F. Ellrich, J. Klier, S. Weber, J. Jonuscheit and G. v. Freymann, "Terahertz Time-Domain Technology for Thickness Determination of Industrial Relevant Multi-Layer Coatings," in *IEEE International Conference on Infrared, Millimeter, and Terahertz Waves*, 2016.

- [27] T. D. Dorney, R. G. Baraniuk and D. M. Mittleman, "Material parameter estimation with terahertz time-domain spectroscopy," *Optical Society of America*, vol. 18, pp. 1562-1571, 2001.
- [28] B. L. Yu, F. Zeng, Q. Xing and R. R. Alfano, "Probing dielectric relaxation properties of liquid CS<sub>2</sub> with terahertz time-domain spectroscopy," *Applied Physics Letters*, vol. 82, p. 4633, 2003.
- [29] R. Storn and K. Price, "Differential Evolution – A Simple and Efficient Heuristic for Global Optimization over Continuous Spaces," *Journal of Global Optimization*, vol. 11, pp. 341-359, 1997.
- [30] M. Nagai, H. Yada, T. Arikawa and K. Tanaka, "Terahertz time-domain attenuated total reflection spectroscopy in water and biological solution," *International Journal of Infrared and Millimeter Waves*, vol. 27, pp. 505-515, 2006.
- [31] A. K. Azad, J. Han and W. Zhang, "Terahertz dielectric properties of high-resistivity single-crystal ZnO," *Applied Physics Letters*, vol. 88, 2006.

## Acknowledgement

I am really appreciated the people who helped me so much in the past three years. I cannot acknowledge them all due to the limit space here.

First of all, I would like to thank my supervisor in Tsinghua University Prof. Wang, Yingxin and Jing, Yingkang. Their expertise, understanding and patience added considerably to my graduate experience. Without his persistence help, I would not finish this work.

Secondly, I would give special gratitude to Prof. Zhao, Ziran. He recommended me to KTH for the dual master study. It was a treasure in my whole life.

Thirdly, Prof. Wacław Gudowski keeps giving me help during the whole dual master program both in KTH and Tsinghua University. He not only helps me with all the study now but also for my future study.

Next, thank to Prof. Fredrik Laurell and Dr. Hoon Jang in KTH Royal Institute of Technology. They gave me a lot of comments to this project.

Moreover, I would like to express the deepest appreciation to Mr. Ding, Guangwei. He helped me a lot with the designation of the experimental setup in his spare time and was very responsible.

I also express my appreciation to my families for their encouragement.

Furthermore, this work would not be possible without the financial aid from China Scholarship Council(CSC).

Finally, my most sincere thanks go to Tsinghua University and KTH for such a great graduate study experience. The experiences have already changed my life.

Thank you.

## Personal Statement

本人郑重声明：所呈交的学位论文，是本人在导师指导下，独立进行研究工作所取得的成果。尽我所知，除文中已经注明引用的内容外，本学位论文的研究成果不包含任何他人享有著作权的内容。对本论文所涉及的研究工作做出贡献的其他个人和集体，均已在文中以明确方式标明。

The author asseverates: this thesis was prepared solely by myself under instruction of my thesis advisor. To my knowledge, except for documents cited in the thesis, the research results do not contain any achievements of any others who have claimed copyrights. To contributions made by relevant individuals and organisations in the completion of the thesis, I have clearly acknowledged all their efforts.

Signature: \_\_\_\_\_

Date: \_\_\_\_\_

## **Resume**

### **Personal Details**

Nationality: Chinese. Place/date of birth: Beijing/ 08-07-1990.

BSc degree in Wind Energy and Power Engineering from North China Electric Power University, 2012, graduating with a very good grade point average.

Master's student in Nuclear Energy and Nuclear Technology Engineering from Tsinghua University, 2015-2018.

Master's student in Engineering Physics from KTH Royal Institute of Technology, 2016-2018.

### **Publications**